INTEGRATED APPLICATION OF PETROPHYSICAL AND GEOPHYSICAL INVERSION TECHNIQUES FOR RESERVOIR QUALITY PREDICTION IN THE CRETACEOUS NANUSHUK FORMATION, NORTH SLOPE, ALASKA

By

Jennafer L. Foreman, B.S.

A Professional Project Report Submitted in Partial Fulfillment of the Requirements

for the Degree of

MASTER OF SCIENCE

in

Applied Geological Sciences

University of Alaska Anchorage

May 2021

APPROVED:

Simon Kattenhorn, Ph.D., Committee Chair
Shuvajit Bhattacharya, Ph.D., Committee Member
Claudia Cannatelli, Ph.D., Committee Member
Simon Kattenhorn, Ph.D., Director
Department of Geological Sciences
John Petraitis, Ph.D., Interim Dean
College of Arts and Sciences
Mary Jo Finney, Ph.D., Dean
Graduate School

Abstract

Recent Brookian discoveries on Alaska's North Slope has re-focused petroleum exploration, redirecting industry interest towards pursuing younger, shallower, often stratigraphically trapped reservoirs of the Nanushuk and Torok formations. In order to effectively and continuously characterize the reservoir properties of these prospective reservoir formations, an advanced, integrated petrophysical and seismic interpretation workflow is needed.

By infusing the post-stack model-based inversion workflow with the results of a detailed petrophysical, the resultant inverted acoustic impedance cube reveals quantifiable reservoir property information based on optimized log-measured data inputs at every trace location across the entire 3D seismic volume. This integrated workflow was applied to the Nanuq South 3D seismic volume to detect quantifiable variations in Brookian reservoir quality across the study area. The low frequency background model used to guide the inversion process was generated based on log-measured data from the Itkillik River Unit 1 well. Drilled in 1978, this well contains data of a quality consistent with the logging technology available at the time and is representative of the type of data available across much of Alaska's exploratory basins.

The integrated inversion workflow generated an inverted impedance volume that successfully detected the Narwhal Sand, a Nanushuk equivalent reservoir penetrated by the Putu 2 and Putu 2A wells, despite failing the majority of the blind well tests. By selecting a well with legacy or vintage data to train the background model, this project demonstrated that seismic inversion can yield meaningful results regardless of the vintage of well data chosen to train the background model.

Table of Contents

Abstract iii
Table of Contents iv
1. Introduction 1
2. Geologic Background 7
  2.1 Arctic Alaska Geologic Context 7
  2.2 The Brookian Petroleum System 15
    2.2.1 Petroleum System Background 15
    2.2.2 The Brookian Petroleum System 19
3. Available Data 22
4. Methods 25
  4.1 Workflow Overview 25
  4.2 Software 26
  4.3 Technical Methodology Background 26
    4.3.1 Basic Seismic Interpretation: Seismic Trace Data and Seismic Attributes 26
    4.3.2 Geophysical Log Properties and Petrophysical Cross-plots 28
    4.3.3 Model-based Post Stack Seismic Inversion 33
5. Results 35
  5.1 Seismic Attributes and Basic Seismic Interpretation [Petrel™] 35
  5.2 Petrophysical Interpretation and Multi-Mineralogical Modeling [PowerLog™] .. 38
    5.2.1 Well Correlation and Petrophysical Analysis 38
    5.2.2 Multi-Mineralogical Modeling 46
    5.2.3 Petrophysical Cross-plots 48
  5.3 Post-Stack Seismic Inversion [HampsonRussell™] 58
    5.3.1 The Forward Model 58
    5.3.2 The Inverse Model 68
6. Discussion 82
7. Conclusions 87
8. Recommendations for Future Work 88
9. References Cited 89

1. Introduction

Historically, oil companies have primarily focused exploration efforts within the Alaska North Slope Petroleum Province on prospects within older, deeper structural plays involving reservoir formations from the Beaufortian and Ellesmerian Sequences (Gregorson and Brown, 2019) (Figure 1.1). Beginning in the early 2000's, with the modernization of seismic imaging technology, exploration on Alaska's North Slope began to shift to younger, shallower, and sometimes stratigraphically trapped prospects. The structurally trapped oil reservoirs of two of the United States' largest oil fields, the Kuparuk River Field's Kuparuk Formation and the Prudhoe Bay Field's Ivishak Formation, are prime examples of successful exploration within these older Beaufortian and Ellesmerian sequences (Figure 1.2).

From 2013 to 2017, four new stratigraphically trapped discoveries targeting Upper Cretaceous reservoirs of the Brookian Sequence were announced, marking a distinct transition in the geologic age and trapping style of regional exploration targets. The primary reservoir intervals for three of these recent discoveries (Willow, Horseshoe, and Pikka) are the shelf margin and shelf edge delta deposits of the Nanushuk Formation, while the primary reservoir interval for the recent Smith Bay discovery are the turbidite and basin floor fan deposits of the Torok Formation (Figure 1.3). According to the most recent assessments published by the United States Geological Survey (USGS) and the Bureau of Ocean Energy Management (BOEM), the Brookian Sequence contains a mean volume of seven to eight billion barrels of undiscovered hydrocarbon resources across multiple land-use areas (NPR-A, State of Alaska, tribal, and Federal-OCS) (Decker, 2018; Houseknecht, 2019).

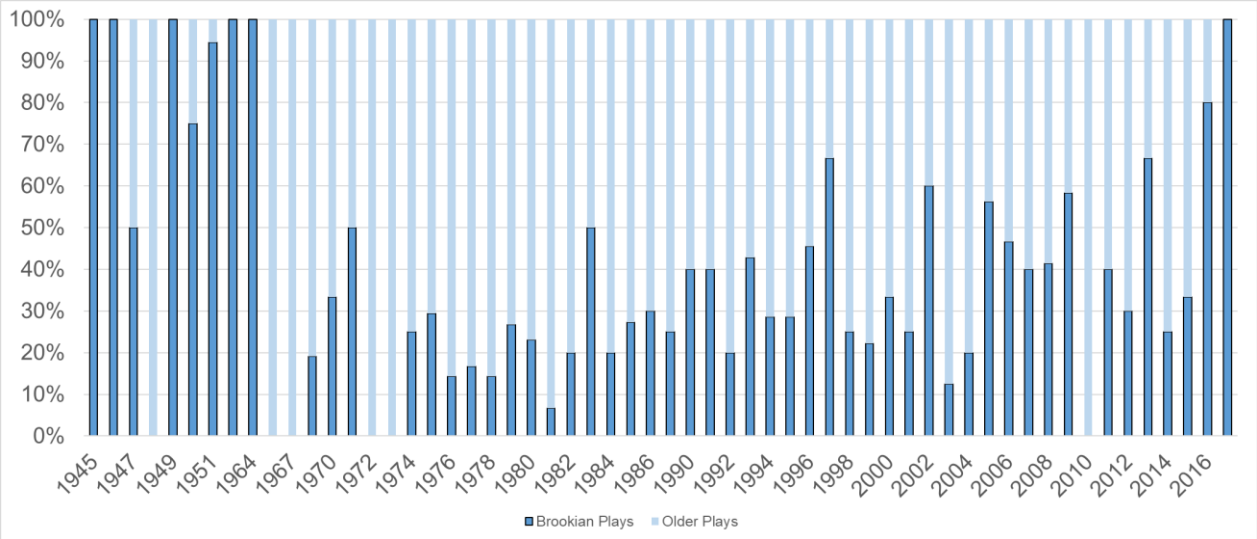

Figure 1.1 Annual percentage of Brookian play exploration targets on the Alaskan North Slope, 1945 to 2017. This chart includes exploration targets that were identified in public well records by the original operator as the intended exploration target for each individual exploration well. A single well may have multiple identified exploration targets. “Brookian Plays” include exploration targeting Brookian interval topset, foreset, and bottomset formations. “Older Plays” include exploration targeting Early Cretaceous or older reservoir formations. Modified from Gregersen and Brown (2019).

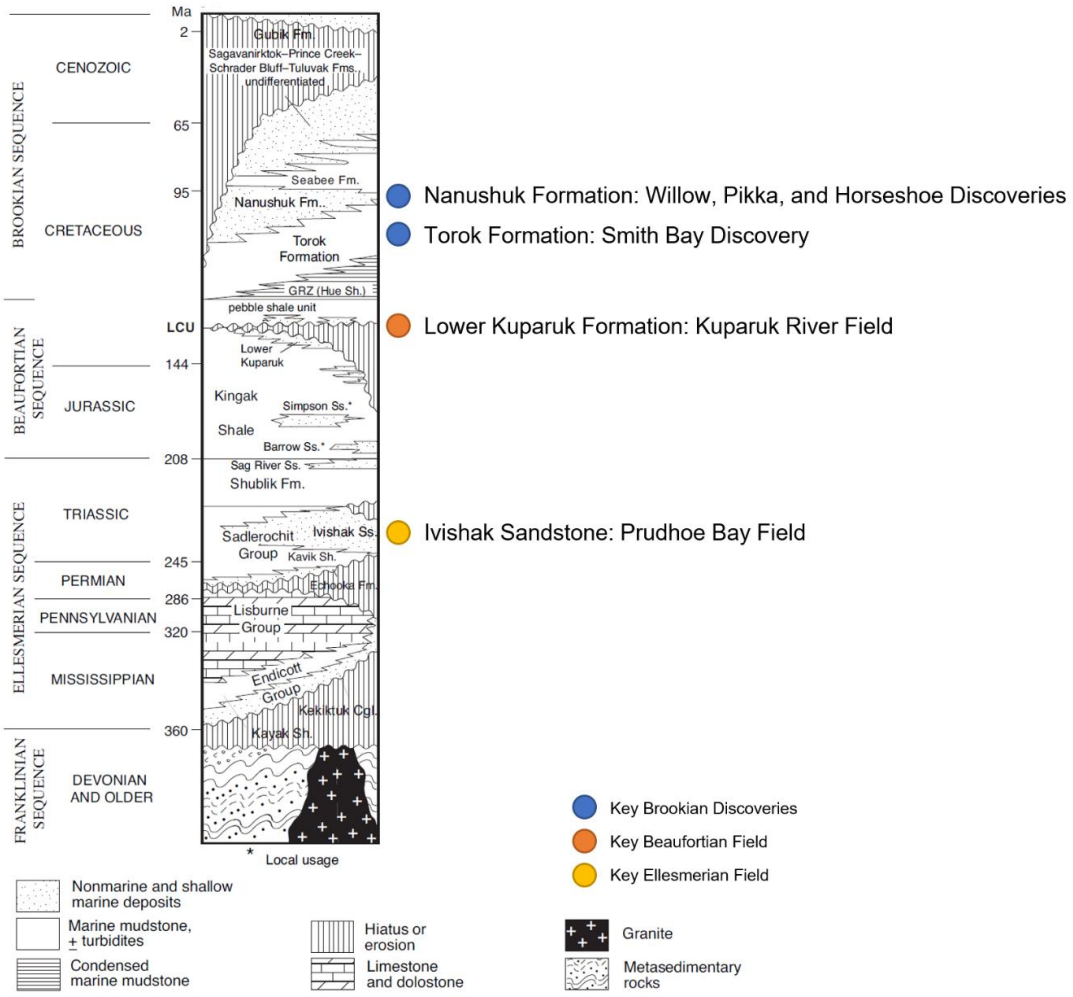

Figure 1.2 Generalized stratigraphic column. The colored icons highlight key stratigraphic intervals and their corresponding discovery or field name. Prudhoe Bay and Kuparuk River Fields, two of the US's top 10 oil fields ranked by total original resource volume, tap into primary reservoir formations which are structurally juxtaposed against non-permeable formations. This mainly structural trapping style is generally easier to identify using legacy seismic surveys and simplified seismic mapping techniques. Modified from Hudson et al. (2006).

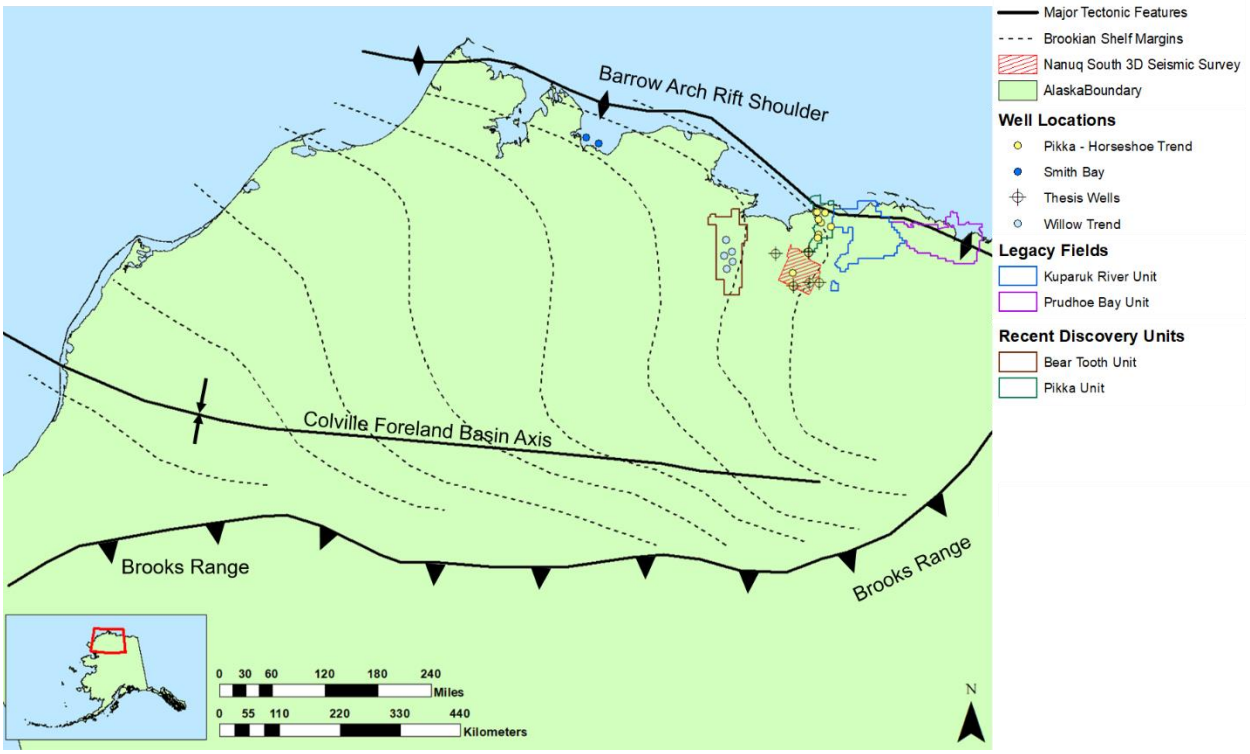

Figure 1.3 Study area overview map. This figure highlights key tectonic elements (solid black), approximate locations of Brookian shelf-edge margins (dashed black), the Nanuq South 3D seismic survey outline (hashed red), field unit outlines (see legend), and well locations (see legend). Paleo-current direction has been demonstrated to be perpendicular to shelf margin trajectories and indicate the primary direction of sediment transport across different portions of the basin (Houseknecht, 2009). Based on the shelf-margin trajectories, the sediment transport direction was primarily west to east across the central Colville foreland basin, southwest to northeast along the northern margin of the Colville foreland basin, and south-southwest to north-northeast along the Brooks Range bounded southern margin of the Colville foreland basin (Houseknecht, 2009) Modified from Decker (2018) and Houseknecht (2019).

Numerous scientists and researchers have studied portions of the Brookian clinothems qualitatively, focusing on sequence stratigraphic interpretation and descriptive integration of 2D seismic interpretation, well log analysis, and core analysis to draw conclusions related to reservoir quality (Homza, 2004; Houseknecht et al., 2009; Helmold, 2016; Houseknecht, 2019). Quantitative techniques used to study the Brookian clinothem package have focused mainly on the trajectory of the paleoshoreline during Brookian deposition and quantitatively measuring clinothem geometry (Ramon-Duenas et al., 2018). Within the Alaskan geologic context, the workflow for joint seismic and petrophysical inversion is not well-established. There have been very few published works attempting to apply an integrated petrophysical and/or quantitative seismic interpretation workflows, namely, seismic inversion, to predict reservoir quality for the Nanushuk and Torok formations. A study published in 2001 demonstrated the effectiveness of an integrated quantitative methodology using data from the Alpine Field, North Slope Alaska (Gingrich et al., 2001). This study applied a joint petrophysical and quantitative seismic inversion methodology to characterize the distribution of favorable reservoir properties of the Upper Jurassic Alpine Formation (Gingrich et al., 2001). In 2020, Bhattacharya and Verma published an article utilizing seismic attributes and petrophsyical analysis to characterize the Nanushuk and Torok Formations, but did not apply a seismic inversion workflow. Compared with a typical exploration workflow leveraging common seismic attributes, integrated seismic and petrophysical inversion results are more insightful because they can be calibrated with core and log data. In

contrast, seismic attributes are not typically calibrated with core and log data, and instead, are based mostly on relative changes in waveform characteristics.

The primary goal of this study was to quantitatively predict areas with favorable Nanushuk and Torok reservoir quality utilizing an integrated petrophysical inversion and seismic inversion workflow. Vintage well data was selected to train the inversion model to demonstrate the effacy of this technique using these legacy data sets. Since much of Alaska's data from earlier phases of exploration and development will be of similar vintage and quality state-wide, if successful, this project intends to provide proof of concept that model-based inversion can provide usable results even when based soley on vintage well data. By leveraging publicly available three dimensional seismic data and legacy Alaskan well data, a quantitative seismic and petrophysical inversion process can delineate areas with quantifiably better reservoir properties (i.e. porosity and relative clay content). This integrated process produced a three-dimensional data volume quantifying acoustic impedance. The impedance cube was then transformed using relationships defined by the petrophysical analysis of available geophysical log data to generate a porosity volume, which can be utilized to further support hypotheses attempting to explain why some locations within the regional study area are more productive than others. Additionally, the results of this integrated petrophysical and seismic inversion workflow can be used to help assess the chance of geologic success of Brookian plays by providing a regional dataset capturing the spatial variations of porosity and relative clay content (lithology) across the study area.

2. Geologic Background

2.1 Arctic Alaska Geologic Context

The Arctic Alaska petroleum province encompasses the following areas: the National Petroleum Reserve of Alaska (NPR-A), portions of the Alaska National Wildlife Refuge (ANWR), and the state and tribal lands between the NPR-A and ANWR. This study focused on the area covered by the Nanuq South 3D seismic survey on the Colville High within the Colville foreland basin in eastern portion of the NPR-A (Figure 2.1).

The regional stratigraphy of the North Slope is divided into four tectonostratigraphic megasequences: the Franklinian, Ellesmerian, Beaufortian, and Brookian (Hubbard et al., 1987) (Figure 2.2 and Figure 2.3). The pre-Mississippian Franklinian Sequence is generally considered the acoustic and economic basement and is composed of sedimentary and metasedimentary rocks (Bird, 2001; Houseknecht and Bird, 2004). The Mississippian to Triassic Ellesmerian Sequence is composed of siliciclastic and carbonate strata and contains proven source rocks (i.e., the Shublik Formation) and proven reservoir rocks (i.e., the Kekiktuk, Lisburne, Ivishak, and Sag River Formations) (Bird, 2001). The Jurassic to Early Cretaceous Beaufortian Sequence is composed of a stratigraphically complex, rift-associated, marine-dominated sediments with sections of locally present sandstones (Bird, 2001). The Beaufortian Sequence contains the regionally present Lower Cretaceous Unconformity (LCU), which cuts down-section towards the Beaufort Shelf, increasingly truncating the Beaufortian source and reservoir rocks from south to north across the study area (Figure 2.3) (Bird, 2001). The Beaufortian contains proven source rocks (i.e., the Kingak Shale and the

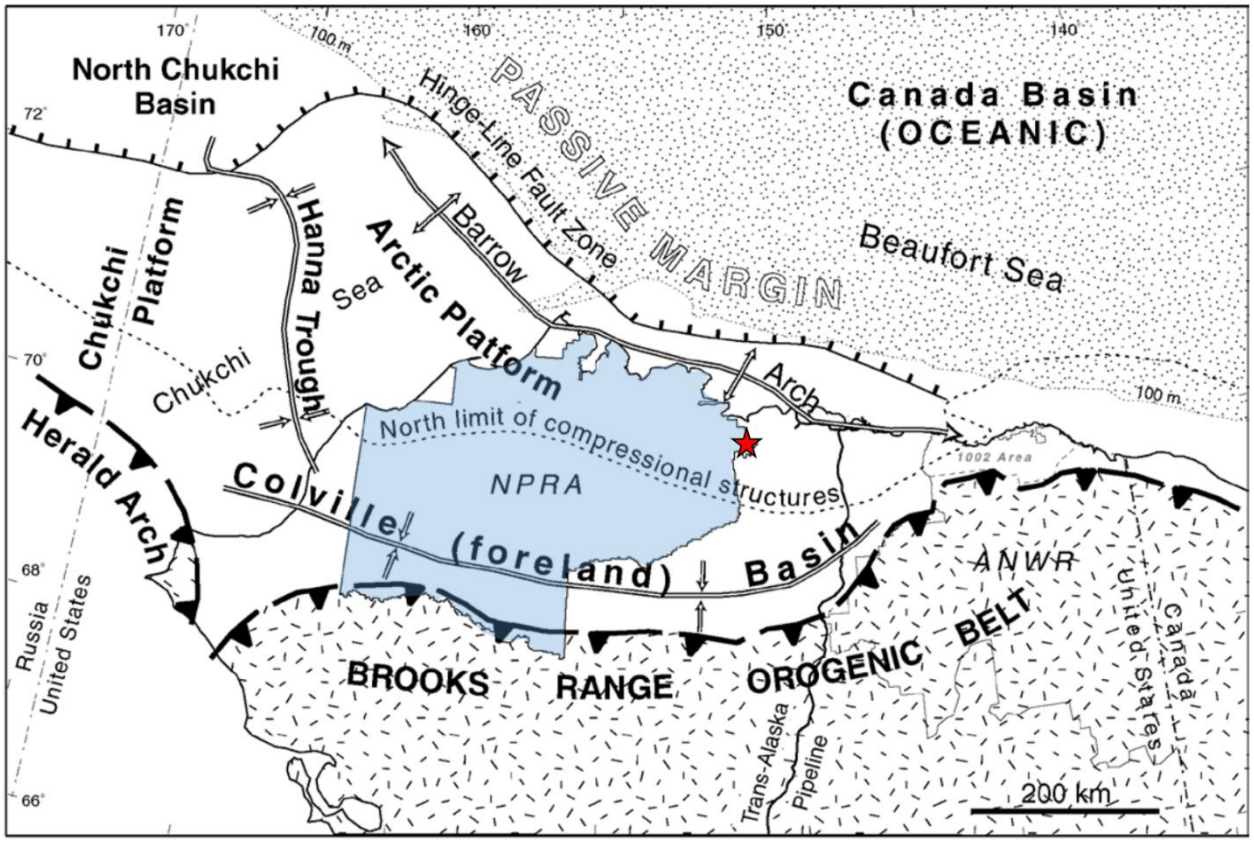

Figure 2.1 Regional map of the Arctic Alaska petroleum province showing the approximate location of the study area (red star) within the Colville foreland basin. The Colville foreland basin is bounded to the north by the Barrow Arch and bounded to the south by the Brooks Range Orogenic Belt. Modified from Bird (2001).

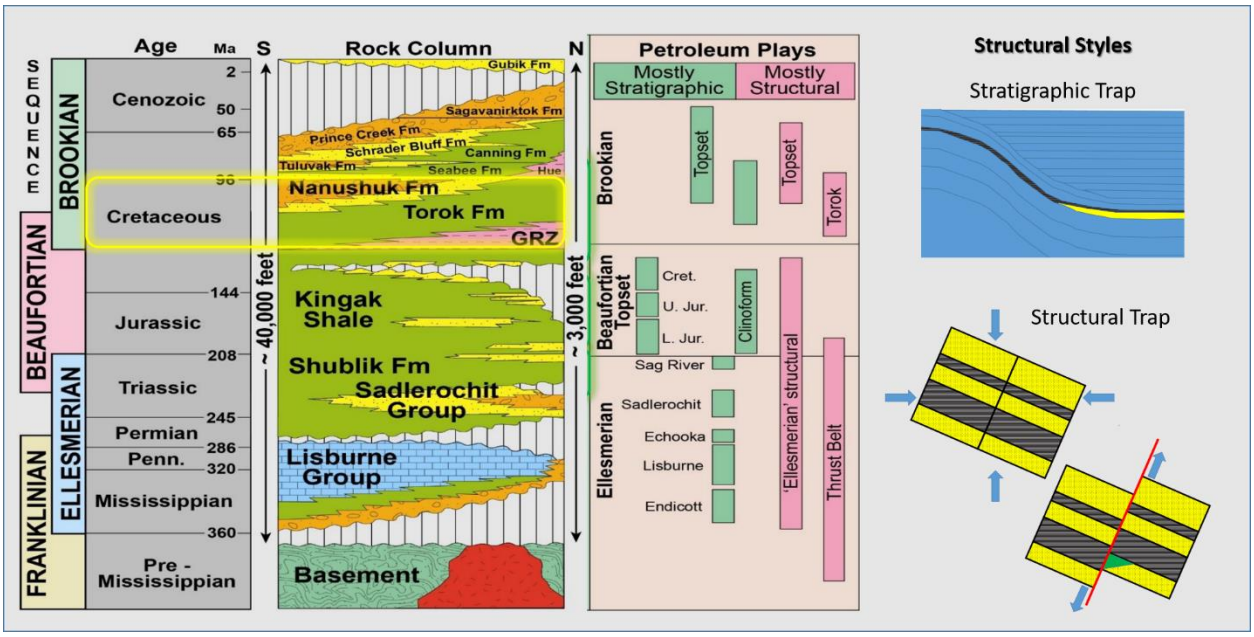

Figure 2.2 North Slope stratigraphic column and petroleum plays. The primary reservoir intervals in the Brookian Sequence are the Cretaceous Nanushuk and Torok Formations. The reservoirs of the Nanushuk Formation Topset Play as encountered in the NPR-A are trapped by stratigraphic or structural trapping mechanisms, with the trapping mechanisms varying across individual accumulations. The reservoirs of the Torok Formation Bottomset Play as encountered in the NPR-A are trapped by structural trapping mechanisms or a combination of stratigraphic and structural mechanisms. Stylized examples of two types of structural styles are illustrated on the right side of this graphic. Modified from Decker (2018).

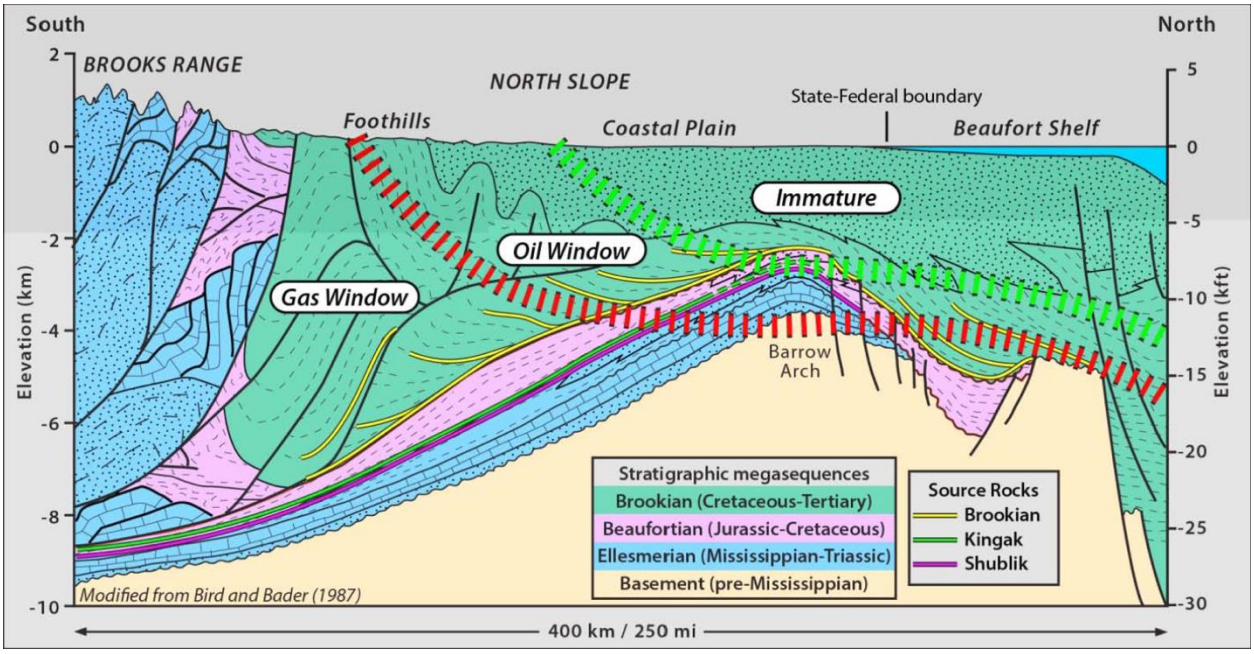

Figure 2.3 Generalized south to north cross-section – Colville foreland basin. This cross-section depicts large structural features, general megasequence geology, maturity windows, and prominent modern features present in the Colville foreland basin. The maturity windows are indicated on the graphic, bounded by green or red hatched lines. The oil window is the area between the red and green lines. Source rocks within the oil window are mature and capable of generating oil. The section above the green hatched line is immature, indicating that source rocks above this depth horizon are not thermally mature enough to produce hydrocarbons. Source rocks below the red hatched line are within the gas window, indicating these rocks are thermally capable of generating gas. This maturity window was estimated using regional vitrinite reflectance data. Modified by Houseknecht (2017) from Bird and Bader (1987).

Pebble Shale Unit) and proven reservoir rocks (i.e., the Kuparuk Formation). The Cretaceous to Tertiary aged Brookian Sequence is composed of clastic sediment derived from the Chukotka and Brooks Range orogens and was deposited in the Colville foreland basin with a thickness exceeding 6000 m (approx. 25,000 ft.) in the deepest portions of the basin (Figure 2.4) (Bird, 2001; Houseknecht, 2019).

This project focuses on the giant Brookian clinothems deposited during the Aptian to Albian time. These clinothem deposits are composed of the gamma ray zone (GRZ) of the Hue Shale, the Torok Formation, and the Nanushuk Formation. The Hue Shale is a source rock unit, composed of a condensed section of distally deposited mudstone seismically expressed as a bottom-set reflector displaying localized interfingering with the time-correlative Torok Formation (Houseknecht and Bird, 2008; Bird, 2001). The Torok Formation preserves the basin floor, toe of slope, slope, and turbidite deposits shedding into the Colville foreland basin (Bird, 2001). The Torok Formation is typically composed of silty mudstone with localized pockets of sandier material related to the turbidite deposits. The Torok Formation is seismically expressed as foreset and bottomset seismic facies within the clinothem package (Houseknecht and Bird, 2008). The Nanushuk Formation is composed of proximal mudstones, sandstones, and coal beds deposited in a range of settings including marine, shelf, fluvial, shore-face deltas, and coastal plain environments (Houseknecht and Bird, 2008). The Nanushuk Formation is seismically expressed as a topset within the clinothem package. Together, the Hue Shale, Torok, and Nanushuk formations represent a third-order depositional sequence, with successive sequences appearing on seismic

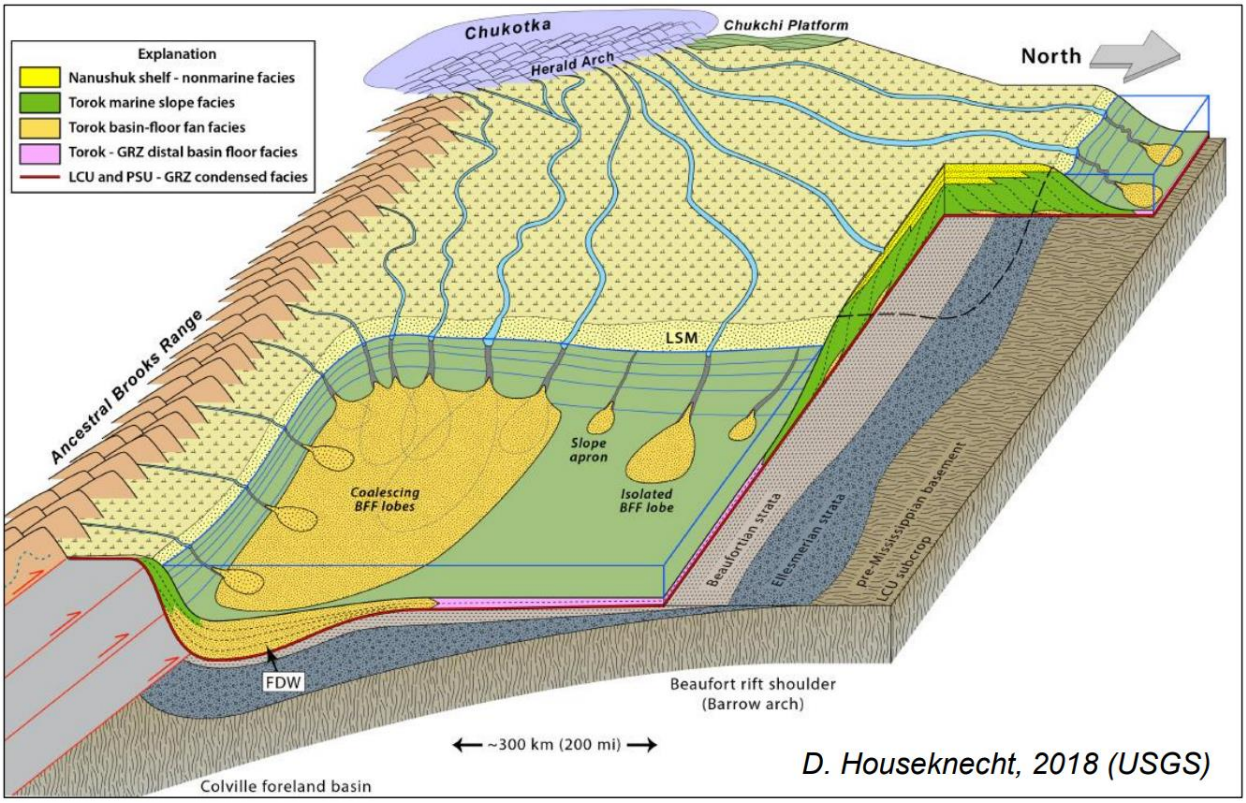

Figure 2.4 Colville foreland basin paleo-depositional model. Note: north is to the right in this figure. This figure illustrates the variety of depositional environments present in the study area during the Brookian. The concept of a bimodal sediment source is depicted, highlighting sediment influx into the Colville foreland basin from the Chukotka uplift in the west and a separate source of sediment influx from the ancestral Brooks Range in the south (Houseknecht, 2019). Sediment from the Chukotka uplift was distributed via the Corwin Delta system, while sediment from the Brooks Rage uplift was deposited via the Umiat Delta system (Houseknecht, 2019).

reflection cross sections as a series of clinoform bounded clinothems stepping west to east across the Colville foreland basin (Figure 2.5).

Observations made by previous authors from seismic and outcrop data regarding paleocurrent indicators within the Brookian Sequence noted that the foreset dip directions could be generally described in three distinct areas (Figure 1.3) (Houseknecht, 2009). Data from the Chukchi and Beaufort Shelf exhibited north to northeast foreset dips (Houseknecht, 2019). Data from across the Colville basin exhibited eastern dipping foresets, except in the southeastern corner of the Colville foreland basin, where foresets dipped to the north and northeast (Houseknecht, 2019). Along the outcrop belt north of the Brooks Range, data indicating a north to northeast paleocurrent direction (Houseknecht, 2019). In each case, the direction of foreset dip is thought to represent the primary direction of sediment transport. Similarly, Houseknecht (2019) also observed that shelf margin trajectories are typically perpendicular to the foreset dip/paleocurrent direction. Houseknecht (2019) further observed that the shelf margin trajectories in the western half of the study area are fairly linear and then transition in the east to a non linear, bending trajectory. Based on these observations, detrital zircon analysis, and building on conclusions and observations published by other authors, Houseknecht (2019) confirms bimodal sediment delivery patterns from two distinct systems: the Chukotka-derived sediment delivered through the Corwin delta system eastwardly across the Colville basin, and the Brooks Range-derived sediment delivered through the Umiat delta system, deposited in a northward direction, proximal to the mountain front (Figure 2.4).

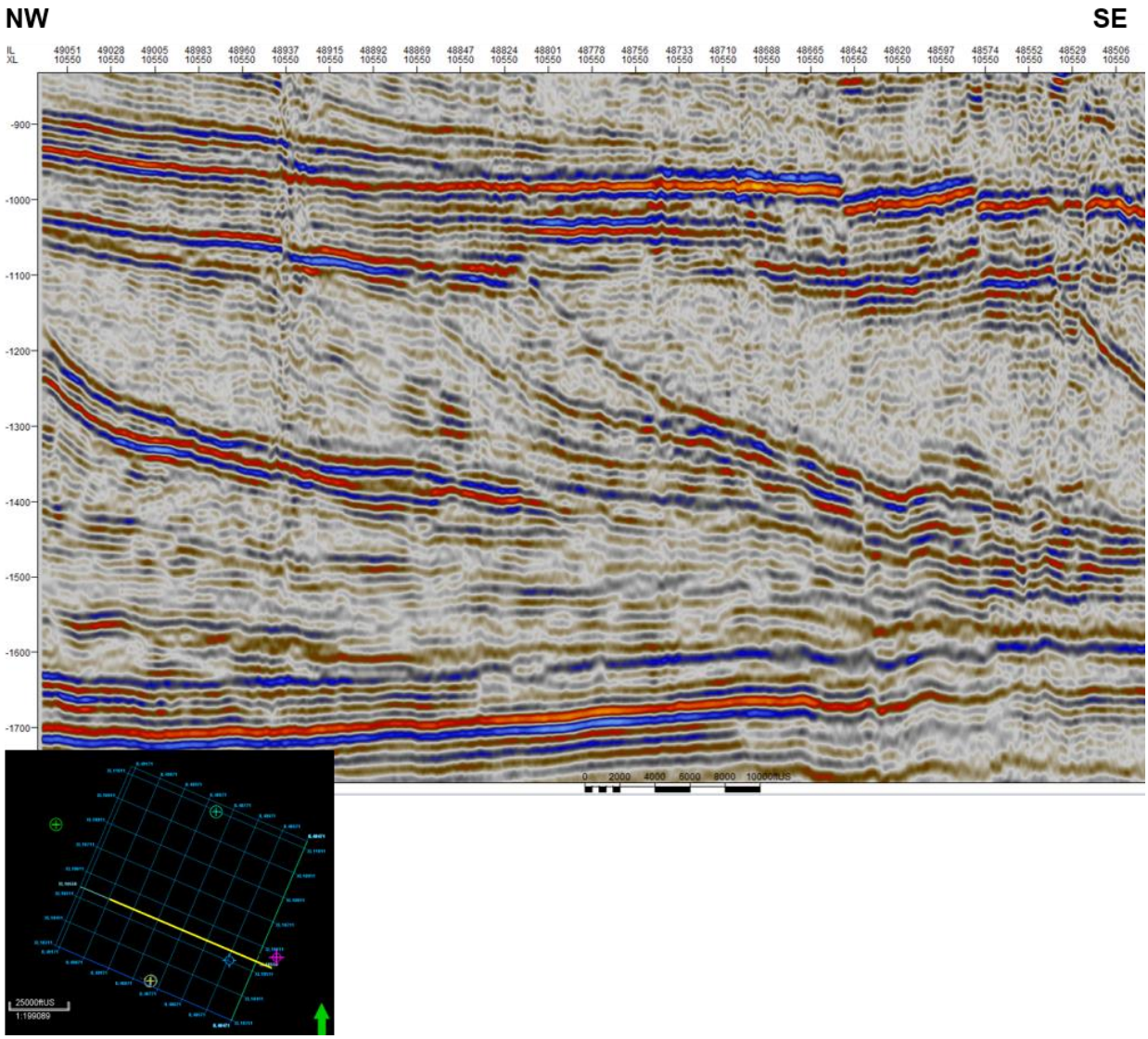

Figure 2.5 Seismic reflection cross-section from Nanuq South 3D seismic survey (State of Alaska, 2017). This NW to SE seismic reflection cross-section (location of cross-section indicated on inset map) illustrates the sigmoidal geometry of the Brookian clinoform surfaces as they step west to east across the Colville foreland basin, recording the history of sedimentary basin fill during the Early Cretaceous.

2.2 The Brookian Petroleum System

2.2.1 Petroleum System Background

Petroleum Systems Background: Systems, Plays, and Prospects

The Arctic Alaska petroleum province has been an active area for oil and gas exploration and development in the state of Alaska for decades. This structurally and stratigraphically complex petroleum province contains multiple productive sedimentary basins. Each North Slope sedimentary basin contains multiple discovered petroleum systems. A petroleum system is defined in an area based on the presence of at least one discovered hydrocarbon accumulation. The individual components within the petroleum system are the charged reservoirs, the group, or pod, of active source rocks charging the reservoirs, and the network of migration pathways within a sedimentary basin. A single petroleum system can contain multiple petroleum plays. A petroleum play is a geologically related group of prospective and/or discovered hydrocarbon fields whose reservoir, seal, and source rock components are spatially oriented in a way that allows for successful hydrocarbon generation, migration, accumulation, and preservation (Sherwod et al., 1998).

The plays described in the arctic Alaskan region represent a range of structural and stratigraphic trapping styles whose individual principal reservoir and seal components were deposited across a range of depositional environments from the Mississippian Period to present day. Structurally trapped plays are plays whose higher porosity reservoir component is juxtaposed against a lower porosity seal component due to subsurface translation typically associated with faulting or folding. Generally, plays and prospects with a structural trapping style are easier to identify and delineate

using legacy seismic surveys and simplified seismic mapping techniques. Stratigraphically trapped plays are plays whose reservoir component is juxtaposed against a lower porosity sealing component due to deposition or erosion. Detailed delineation of stratigraphically trapped plays often requires a more advanced seismic interpretation workflow, like a model-based post-stack seismic inversion workflow, to fully characterize the reservoir.

A single petroleum play can contain numerous petroleum prospects. A petroleum prospect is defined as an individual accumulation within the larger scale play boundary. Prospect and play delineation is at the core of all exploration activities. Exploration companies searching for the next big hydrocarbon discovery want an accurate assessment of potential hydrocarbon volume to justify spending money leasing acreage. Government agencies regulating the petroleum industry also spend a lot of time and resources on assessing resource volume at the prospect, play, and basin scale to ensure a fair return to the the American people for exploration activities carried out in publicly held acreage.

2.2.1.1 Petroleum System Assessment

Three petroleum system processes (generation, migration, and preservation) must occur and three main petroleum system elements (source, reservoir, and seal) must exist in order for hydrocarbons to accumulate in a system. Each of these components has unique ideal physical rock properties and unique ideal relative clay contents that contribute to the ideal composition of a working conventional petroleum system: source rocks ideally have a high percentage of total organic carbon and are typically rich in clay minerals; reservoir rocks ideally have high porosity, high

permeability, and are poor in clay minerals; and cap rocks ideally have low permeability and are rich in clay minerals (White, 1988; Magoon, 1992). In order for a source rock to generate hydrocarbons, the source rock must have had adequate organic content and reached the necessary temperature to generate hydrocarbons. In the case of conventional reservoirs, the generated hydrocarbons must then be expelled from the source rock and migrate along migration pathways until the flow is impeded by an impermable seal, and an accumulation forms. The seal must be adequately maintained over geologic time in order for the hydrocarbon accumulation to be preserved.

When geoscientists assess a petroleum play or prospect for potential undiscovered resource volume, they often employ a probabilistic resource assessment methodology, examining each individual component and process within the petroleum system to determine the likelihood that the evaluated play or prospect contains trapped hydrocarbons (Rose, 1991 and Sherwood et al., 1998). Petroleum system assessment methodologies can be applied at varying scales (play and prospect) to quantify the volume of undicovered conventional resources contained within the evaluated play or prospect.

While the specific detailed methodologies employed vary from organization to organization, most methodologies involve an exercise in ascertaining the probability of geologic success (P_g or $P_{geologic}$) of the petroleum play or prospect (White, 1988; Sherwood et al., 1998). This P_g is determined by assessing the probability of success of the individual petroleum system components (P_{source}, $P_{reservoir}$, and P_{seal}) within the play or prospect being assessed. The probability of geologic success of the play or prospect is the product of the probabilities of success of the individual petroleum system

compoents and is expressed as a fractional percentage (Rose, 1992) (Equation 2.1).

$$P_{Geologic} = P_{Source} \times P_{Reservoir} \times P_{Seal}$$ (Equation 2.1)

As an example, if during an assessment exercise, the source component of a play is assinged a P_{Source} of 1 (100%), this indicates that the assessor has complete confidence based on the available data in the existence and effacy of the evaluated source rock (Sherwood et al., 1998). Similarly, if an individual petroleum system component of a play is assigned a 0% probability of geologic success, this indicates that the assessor has complete confidence based on regional data that there is no possibility for the component to function as intended in the assessed play (Sherwood et al., 1998). It is important to note that while exploration failures do not translate to 0% chance of geologic success, if hydrocarbons are actively being produced out of a petroleum play, then the entire play is “proven”, and thus has a P_g = 100%.

Equation 2.1 demonstrates that the probablity of geologic success of the assessed unit is governed by a principal of all or nothing. In other words, if one process or component fails ($P_{component}$ = 0), then the entire assessed unit fails. For example, if a play has one potential source rock interval but the source rock has never reached thermal maturity, the rock characteristics of your reservoir are irrelevant, since there are no hydrocarbons available for storage.

The value assigned for the probability of geologic success describes the level of certainty that the assessor has based on their evaluation of available geologic and geophysical data that an individual petroleum system component is present and has the

appropriate rock properties to serve its intended function in-place in the assessment area at the assessed scale. Petroleum systems data that are typically analyzed to support a regional probablistic resource assessment methodology include gravity and magnetics data, seismic data, geochemical data, geophysical well log data, and interpretation products such as seismic atrribute cubes, inverted impedance cubes, and petrophysical modeling results. Regional datasets with the potential to quantify key reservoir properties including porosity and rock type are extremely useful in a resource assessment methodology.

2.2.2 The Brookian Petroleum System

The Brookian petroleum system has multiple, proven source rock intervals. The pod of proven source rocks relevant to this study include the Triassic Shublik Formation, the Jurassic Lower Kingak Formation, and the Lower Cretaceous Pebble Shale Unit (PSU) to the Gamma Ray Zone (GRZ), inclusive of the Hue Shale. The Hue Shale is a source rock unit, composed of a condensed section of distally deposited mudstone seismically expressed as a bottom-set reflector displaying localized interfingering with the time-correlative Torok Formation (Houseknecht and Bird, 2008; Bird, 2001).

Regionally, oil generation began during the Early Cretaceous in the Colville foreland basin and reached the Barrow Arch by the Latest Cretaceous to Early Paleogene (Houseknecht, 2018). Vitrinite reflectance (VR) data suggests that the Shublik and Kingak formations are in the oil window across the study area, while the maturity of the PSU-GRZ ranges from immature near the Barrow arch progressing to the oil window in portions of the Colville foreland basin, further maturing to the south where the source rock zone enters the gas window (Figure 2.3) (Houseknecht, 2018).

Sand-prone or clay-poor potential reservoir facies exist in both the Nanushuk and Torok Formations, but more favorable reservoir properties (higher porosity and permeability) typically found within the Nanushuk Formation (Figure 2.2) (Decker, 2018). The Nanushuk Formation is composed of proximal mudstones, sandstones, and coal beds deposited in a range of settings including marine, shelf, fluvial, shore-face deltas, and coastal plain environments (Houseknecht and Bird, 2008). The Torok Formation preserves the basin floor, toe of slope, slope, and turbidite deposits shedding into the Colville foreland basin (Bird, 2001). The Torok Formation also has potential for sand-rich material preservation within turbidite, basin floor fan, slope apron, and slope channel deposits (Houseknecht, 2018). For both the Nanushuk and Torok intervals, prospective clay-poor reservoir material would be overlain by successive silt-rich or clay-rich sedimentation deposited during the subsequent marine transgression, forming reliable local and regional seals over geologic time across the sedimentary basin.

Structural traps are associated with both the Nanushuk and Torok formations, but stratigraphic traps are primarily associated with the recently discovered Nanushuk accumulations (Figure 2.2). The ideal configuration of a successful Nanushuk reservoir is typically a stratigraphically trapped shelf-edge delta deposit that is subsequently flooded by the next transgressive clay-rich sequence. These shelf-edge deposits are generally thick accululations of reservoir quality material perched at the edge of the paleo-slope-shelf break.

There are four proven petroleum plays involving the Nanushuk and Torok formations as defined within the Colville foreland basin: the Nanushuk topset stratigraphic play, the Nanushuk topset structural play, the Torok bottomset structural

play, and the Torok bottomset combination play. The recent discoveries at Willow and Pikka-Horseshoe have tested and proven the basal, stratigraphically trapped Nanushuk Play. (Houseknecht, 2018). Recent exploration wells drilled by Caelus Energy in Smith Bay tested and confirmed the northern extent of the Torok combination play, encountering potential reservoir material within the Torok section, but the company has yet to publicly release well test data to back up their oil-in-place estimates.

3. Available Data

This project integrated multiple types and multiple scales of subsurface geologic and geophysical datasets, including 3D seismic, geophysical well logs, and core data. Vertical resolution is generally in the 30-91 cm (1-3 ft.) range for conventional well log data, while vertical resolution for core data is down to 1.27 cm (0.5 in.). Typical values for the resolution of seismic surveys vary based on the frequency of the source, acoustic properties of the area being imaged, and the acquisition design, but typical resolution for deep penetration seismic is on the order of 10-15 m (32-50 ft.).

The Nanuq South 3D seismic survey was selected for this study and was made available as part of Alaska's tax credit seismic program (Figure 3.1) (State of Alaska, 2017). The Nanuq South 3D survey was acquired in 2004 by Veritas for ConocoPhillips Alaska. This survey covers approximately 300 km^2 (115 mi^2) on the Alaska North Slope with data spread across 1,733 cross-lines and 1,240 in-lines. This survey encountered some issues imaging the subsurface beneath the study area's numerous ice lakes due the low velocity anomaly that exists beneath the perennial water bodies/ice lakes, but the general data quality is more than acceptable for advanced geophysical interpretation techniques (WesternGeco, 2004).

The wells included in this study are the Itkillik River 1, Cronus 1, Flat Top 1, Horseshoe 1, Horseshoe 1A, Putu 2, and Putu 2A wells (Figure 3.1). These seven wells were selected based on their location relative to the selected seismic survey area. Operator acquired well log data, including conventional logs such as gamma (GR), resistivity (RES), neutron porosity (NPHI), bulk density (RHOB), photoelectric (PE), and sonic (DT) were used to perform petrophysical analysis for each well in this study. Core

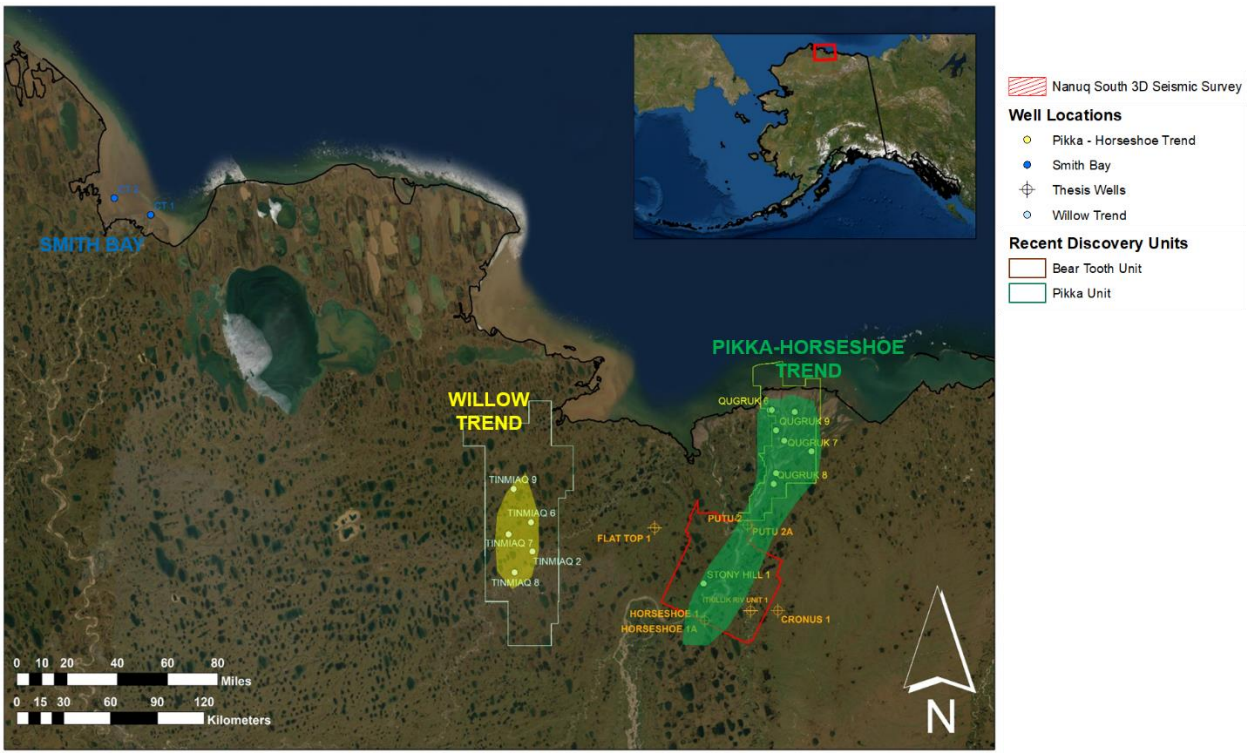

Figure 3.1 Study area basemap. The discovery wells for the Willow, Pikka-Horseshoe, and Smith Bay areas are labeled in yellow, green, and blue respectively. The study wells are displayed in orange. The Nanuq South 3D Survey area is outlined in red. (Alaska Geologic Materials Center, 2019; Alaska Department of Natural Resources Division of Oil and Gas, 2021; ESRI, 2021)

measured data was available for a few of the study wells, so measured core porosity, core permeability, and core fluid saturation data was integrated when available.

Formation tops from the Alaska Oil and Gas Conservation Commission (AOGCC) were used as a starting point to guide well log correlations across the area, though subsequent adjustments were made based on interpretative regional correlation.

4. Methods

4.1 Workflow Overview

The workflow for this post-stack inversion project followed a standard methodology, beginning with the basic interpretation of 3D seismic data, followed by standard log correlation, basic petrophysical analysis, and statistical multi-mineralogical modeling. Next, forward modeling yielded a synthetic seismic trace generated by convolving a respresentative wavelet extracted from the post-stack data with the reflectivity series generated from the log-measured density and P-wave velocity measurements taken at the Itkillik River Unit 1 well location. This relationship between the reflectivity and impedance was then inversely propagated through the volume, resulting in the generation of the inverted, three-dimensional P-wave impedance volume. Within this volume, each individual seismic trace relays information about the actual rock properties at each individual trace location throughout the 3D volume. The inverted trace data can be manipulated to return absolute values of velocity, density, acoustic impedance, and porosity at every trace throughout the survey volume. Blind wells were inserted into the impedance volume as a validation step to check the results. Finally, the petrophysically derived relationship between impedance and porosity was used to generate a reservoir property cube for visualizing porosity and approximating lithology based on relative clay richness.

The Itkillik River Unit 1 well was chosen as the basis for the background model used to perform the post stack inversion due to its vintage, quality of data, and location. Drilled in 1972, this vintage of well data is representative of the data quality resulting from the technology available during the early phase of oil and gas exploration in

Alaska. Well data of similar vintage and quality is present across many Alaskan basins, and in some cases is the only data available in the local area. By selecting an older well like the Itkillik River Unit 1 well with geophysical logs measured with 1970's era tools, this project can serve as proof of concept that modern model-based seismic inversion can be trained using legacy well data and produce a valid, useful result. Additionally, at its closest proximity to the edge of the seismic survey, the Itkillik River Unit 1 well location is approximately 9.25 km (5.75 mi) from the eastern survey boundary. This distance is well within the ideal area of the seismic survey, where the seismic data quality is not impacted by undesirable tapered edge effects (WesternGeco, 2004; Chaouch and Mari, 2006).

4.2 Software

All horizon interpretation and three dimensional seismic visualization was performed using Schlumberger's Petrel™ software package. Well log loading and petrophysical analysis, interpretation, cross-plotting and modeling were performed using CGG's Powerlog™ software package plus an added CGG StatMin™ module. Seismic inversion and 3D property modeling were performed in CGG's Hampson Russell™ software package using the Wells™, Strata™, and Emerge™ modules. All spatial data was processed using ESRI's ArcMap™ software package.

4.3 Technical Methodology Background

4.3.1 Basic Seismic Interpretation: Seismic Trace Data and Seismic Attributes

Three dimensional reflection seismic surveys record the acoustic response of the subsurface. Changes in bulk rock density primarily influenced by spatial variations in pore fluid content, porosity, rock type, mineralogy, and compaction cause seismic

energy to speed up or slow down while traveling from the energy source, through the subsurface, and back to the reciever(s) during seismic acquisition. Spatial variations in the acoustic response of the subsurface are recorded by the receivers and processed to be stored as a three dimensional volume of reflectivity trace data. These seismic reflectivity traces record the spatial location of boundaries between subsurface layers with differing acoustic impedance responses. Acoustic impedance is the product of the layer's density and velocity and as such, changes in pore fluid, compaction, porosity, and other key rock properties affect the relative impedance of stacked layers.

As seismic energy travels from a high impedance layer to a layer with lower acoustic impedance, the acoustic energy will reflect from the interface between the two layers, and be represented by a trough on the seismic section, assuming American polarity. When acoustic energy travels from a low impedance layer to a high impedance layer, this is represented by a peak on the seismic section. The peaks and troughs of an individual seismic trace represent the approximate subsurface locations of impedance layer boundaries.

A seismic section is a series of continuously plotted seismic traces across the survey volume. Horizons are interpreted throughout the seismic section by connecting related peaks and troughs to form a spatially referenced representation of the geometry of that layer or interface across the entire survey volume. Seismic attributes are generated using mathematical relationships that can illuminate structural features, stratigraphic features, and other features of interest (Chopra and Marfurt, 2005). The root-mean-squared (RMS) amplitude attribute, an industry standard attribute, measures the magnitude of the variation of the acoustic impedance over the sampled interval

(Chopra, 2007). This attribute is useful because it highlights areas of high amplitude, which can be utilized as a direct hydrocarbon indicator (DHI), though relying solely on RMS amplitude as a DHI has lead to many dry holes.

4.3.2 Geophysical Log Properties and Petrophysical Cross-plots

Geophysical well logs are continously recorded (or induced) by downhole logging equipment inserted into the borehole either while the borehole is being drilled (logging while drilling) or inserted into the borehole after a section of well has been drilled, but before casing has been set for that interval (open hole logging), Logging equipment can also be deployed in a cased hole, but log data from cased hole runs were not used in this project. Table 4.1 lists the types of geophysical well logs used in this project, the common curve pneumonic, measurement units, primary use, and briefly describes how the tool operates (Rider and Kennedy, 2011). An important thing to note is that geophysical rock properties measured at the well scale are directly relatable to rock properties detectable by seismic data, and thus, the inverse-modeled rock properties can act as a sensitivity and ambiguity tool in the overall inversion process (Chaveste and Hilterman, 2007).

Additional log properties were calculated based on standard petrophysical relationships in prepration for petrophysical cross-plotting, statistical mineralogical modeling, and petrophysical analysis. Table 4.2 lists the complete set of petrophysical properties generated for each well in this project, and includes a list of common abbreviations, the equation used to calculate the transformed log, identifies the log inputs and constants used in the equations, and identifies the primary use of each transformed or calculated log property (Rider and Kennedy, 2011). These log properties

Curve	Log Name	Units	Primary Use	Tool Description
GR	Gamma Ray	gAPI	Rough Lithology, Correlation Log	Meaures the natural radiactivity of the section
RESD	Deep Resistivity	ohm-m	Pore Fluid	Measures the section ability to conduct electrical signals by transmitting an electric signal and measuring the conducted response with an offset receiver.
NEUT, NPHI, φ_N	Neutron, Neutron Porosity (NPHI)	Neutron porosity units	Porosity, Lithology	Record of the section's response to neutron bombardment, related to the section's Hydrogen Index (HI). HI is an indication of the formation's richness in hydrogen.
DEN, DENS	Density	g/cc	Porosity, Lithology, Pore Fluid	Record of the section's bulk density (function of lithology, compaction, and pore fluid)
DT	Sonic Slowness	µs/ft or µs/m	Lithology, Pore Fluid	Measures the acoustic nature of the section by genarting a sound pulse and measuring how long an offset receiver takes to register the pulse.
DTC	Compressional Sonic Slowness	µs/ft or µs/m	Lithology, Pore Fluid	Full Waveform Sonic Tools/Dipole sonic: Measures the slowness of compressional wave arrivals
DTS	Shear Sonic Slowness	µs/ft or µs/m	Lithology, Pore Fluid	Full Waveform Sonic Tools/Dipole sonic: Measures the slowness of shear wave arrivals
PE, PEF	photoelectric factor	barns	Lithology	Record of the photoelectric absoprtion cross-section index,dependent on the atomic complexity of the section

Table 4.1 Geophysical well logs from the original log suites.

Calculated Petrophysical Properties			Inputs		Primary Use
Abbreviation	Desciption	Equation	Curve(s)	Constants	
ρ_{Gar}	Gardner's Equation for Density	$\rho = \alpha V_P^{\beta}$	V_P	$\alpha = 0.31$ $\beta = 0.25$	Lithology Indicator, Porosity, Gas Indicator
DPHI, φ_D	Density Porosity	$\varphi_D = \frac{\rho_{ma} - \rho_{log}}{\rho_{ma} - \rho_{fl}}$	DENS (ρ)	ρ_{ma} = 2.65* ρ_{fl} = 1*	Porosity
PHIA, φ_{avg}	Average Porosity	$\varphi_{avg} = \frac{\varphi_N + \varphi_D}{2}$	DPHI (Φ_D), NPHI (Φ_N)		Porosity
V_{SH} ,IGR	Shale Volume, Gamma Ray Index	$IGR = \frac{GR_{LOG} - GR_{Clean}}{GR_{Shale} - GR_{Clean}}$	GR	GR_{Clean}, GR_{Shale} taken from interval of interest	Clay content
$V_{SH(Lar\_Old)}$	Shale Volume (Larionov Old Rocks)	$VSH_{LAR} = 0.33(2^{2\,IGR} - 1)$	IGR		Clay Content in old rocks
V	Velocity	$V = \frac{1}{DT \times 10^{-6}}$	DT		Lithology, Compaction, Pore Fluid
V_P	P-Wave Velocity	$V_P = \frac{1}{DT_C \times 10^{-6}}$	DTC		Lithology, Compaction, Pore Fluid
V_S	S-Wave Velocity	$V_S = \frac{1}{DT_S \times 10^{-6}}$	DTS		Lithology, Compaction, Pore Fluid
V_PV_S	V_PV_S Ratio	$V_PV_S = V_P \times V_S$	V_p, V_s		Pore Fluid, Lithology, Compaction
Z, AI	Acoustic Impedance	$Z = AI = \rho \times V$	DENS (ρ), DT		Pore Fluid, Lithology, Compaction
Z_P, AI_P	P-Wave Acoustic Impedance	$Z_P = AI_P = \rho \times V_P$	DENS (ρ), DTC		Pore Fluid, Lithology, Compaction
Z_S, AI_S	S-Wave Acoustic Impedance	$Z_S = AI_S = \rho \times V_S$	DENS (ρ), DTS		Pore Fluid, Lithology, Compaction
$S_{w(Archie)}$	Archie's Water Saturation	$S_w{}^n = \frac{R_w}{(\varphi^m \times R_t)}$	RES(R)	R_w, a, m, n based on Pickett Plot	Pore Fluid
$S_{w(Simandoux)}$	Simandoux Water Saturation	$\frac{1}{RES} = \frac{\varphi^m S_w{}^n}{a\,R_W} + \frac{V_{SH}S_W}{R_{Shale}}$	RES(R)	R_w, a, m, n based on Pickett Plot, R_{sh} from shale zone	Pore Fluid (Shaly Section)

Table 4.2 Petrophysical log transformations.

are evaluated and used to make interpretations regarding the lithology, clay content, porosity, pore fluid content, mineralogy, and compaction of the measured interval.

Petrophysical cross-plotting was then used as a way to visually inspect related data sets for trends and data problems. Table 4.2 lists the petrophysical cross-plots generated and analyzed for each well in this project and lists the most common use for each cross-plot (Rider and Kennedy, 2011). In general, petrophysical cross-plot analysis is used to visually determine rock type, identify relationships between data sets, visually determine water saturation, in addition to functioning as a data quality control tool. Cross-plots are generally most impactful when the data visualized is limited to a single formation or zone.

Key Petrophysical Cross-Plots (Y vs X, colored by Z)				
Short Name	**X Variable**	**Y Variable**	**Z Variable**	**Application**
Pickett Plot	Resistivity	Average Porosity	Gamma Ray	Determining Water Resistivity
N-D	Neutron Porosity	Density	Shale Volume	Lithology Indicator, Gas Effect
φ vs Z_p	P-Wave Impedance	Average Porosity	Shale Volume	Regression Equation used to generate Porosity volume
Z_p vs S_{hc}	Hydrocarbon Saturation	P-Wave Impedance	Shale Volume	Regression Equation used to generate Fluid Saturation volume
ρ vs φ	Porosity	Density	Shale Volume	Demonstrates inverse relationship, high porosity = low density
Vp vs φ	Porosity	P-Wave Velocity	Shale Volume	Demonstrates inverse relationship, high porosity = low velocity

Table 4.3 Petrophysical cross-plots and their common uses.

4.3.3 Model-based Post Stack Seismic Inversion

CGG's Hampson Russel™ software package was used to conduct the seismic inversion methodology described earlier in this section. Hampson Russell™ offers four main general algorithms for performing post-stack seismic inversion: model-based, bandlimited, colored inversion, and sparse spike. The method selected for this project is a model-based seismic inversion algorithm with a full spectrum output of absolute impedance values. The background model is a low frequency model generated using input well data, a wavelet extracted from the original trace data, and a series of regional horizons (Russell and Hampson, 1991). When computing the impedance volume, the computer program attemps to generate a blocked modeled velocity log at each trace location using the input horizons to constrain the extent of the blocked logs (Russell and Hampson, 1991). These modeled velocity logs are matched to synethetics generated at each well identified as a model input, and the modeled layers are adjusted to improve the fit of the model to both the well data and the horizon data (Russell and Hampson, 1991). Once the final model is generated, it can used in the inversion process, acting as a geologic roadmap for the inversion algorithm. The inversion process can be applied to the entire trace volume, with options to apply a soft or hard contraint when considering the background model. Upon completion, the inversion process generates an inverted impedance volume from the original seismic trace data, based on the low frequency geologic roadmap provided by the background model. In an effort to reduce computational run times for the inversion process, the inversion was only performed over the interval of interest, ensuring that an interpreted horizon bounded the top and bottom of the inversion window (752ms to 1552ms). The resulting inverted impedance

volume contains an impedance trace generated at every point, such that the inverted impedance trace records quantitatively the spatial variations of velocity and density continuosuly at every point in the entire 3D volume (Russell, 2017).

5. Results

5.1 Seismic Attributes and Basic Seismic Interpretation [Petrel™]

Log-measured velocity data (checkshot, dipole sonic, or VSP) was used to generate an “on the fly” time-depth relationship (TDR) for each project well. This relationship established a tie between the well data, which is recorded in the depth domain, and seismic data, which is recorded in the time domain (Figure 5.1). This TDR established a first pass well to seismic tie, which assisted in performing horizon interpretation in the seismic data volume. A more detailed well-seismic tie was performed later in the project for all project wells.

Once the initial TDR was established, Nanushuk and Torok formation tops from the AOGCC were posted on a well cross section with seismic panels and edited as needed to reflect the true stratigraphy of the basin. The adjusted formation tops were picked and correlated across all project wells. Six horizons representing individual clinoform surfaces were mapped on one of every fifty in-lines and one of every fifty cross-lines using the AOGCC formation tops at individual well locations as the starting point. Surfaces were generated for each horizon, such that the horizons was continuously mapped throughout the survey area (Figure 5.2). These surfaces were then used as input to guide the forward modelling process, generate the background model, and ultimately influence the inversion results, focusing the process along intervals of interest.

Complex trace attributes (RMS Amplitude and sweetness) were computed for the whole seismic volume as a check to verify that the Nanuq South 3D seismic data set contained enough preserved amplitude information for the seismic inversion process to

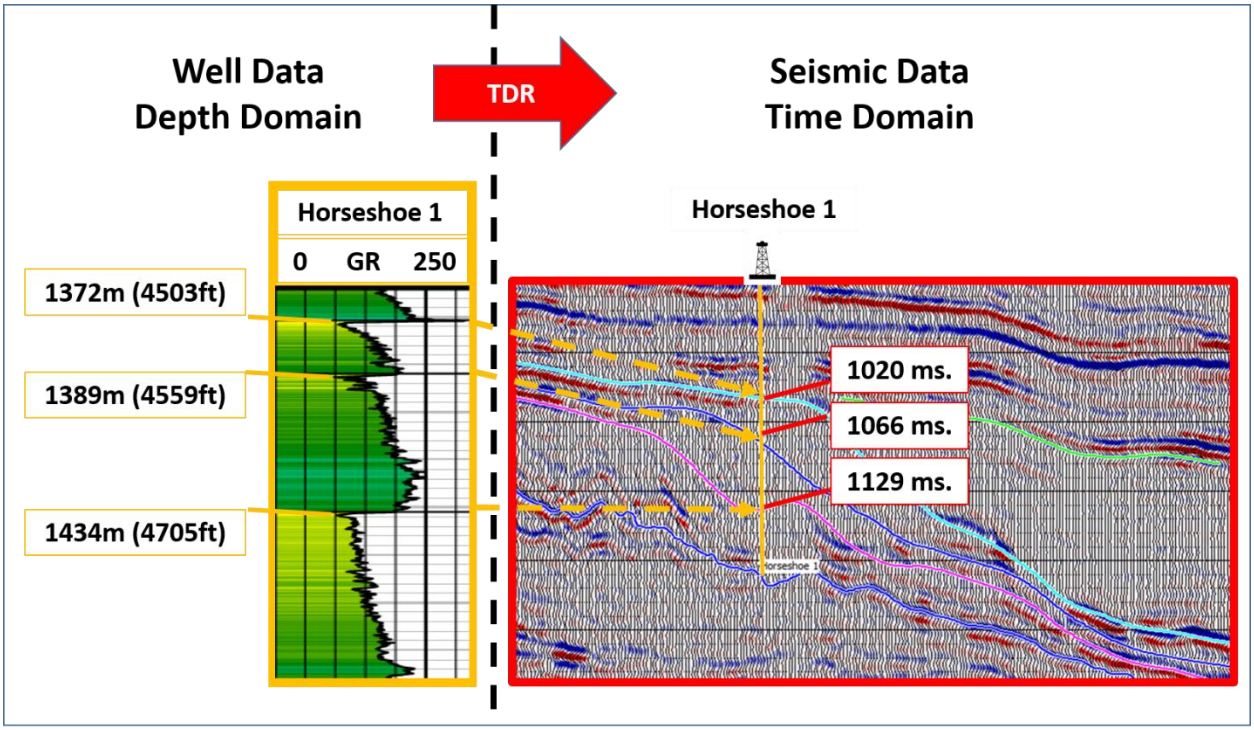

Figure 5.1 Time-depth relationship (TDR). This figure illustrates the goal of establishing a TDR between log-measured well data measured in the depth domain and seismic data from a post-stack seismic reflection survey measured in the time domain. This figure is for illustrative purposes only, and does not depict the true results of the well-tie.

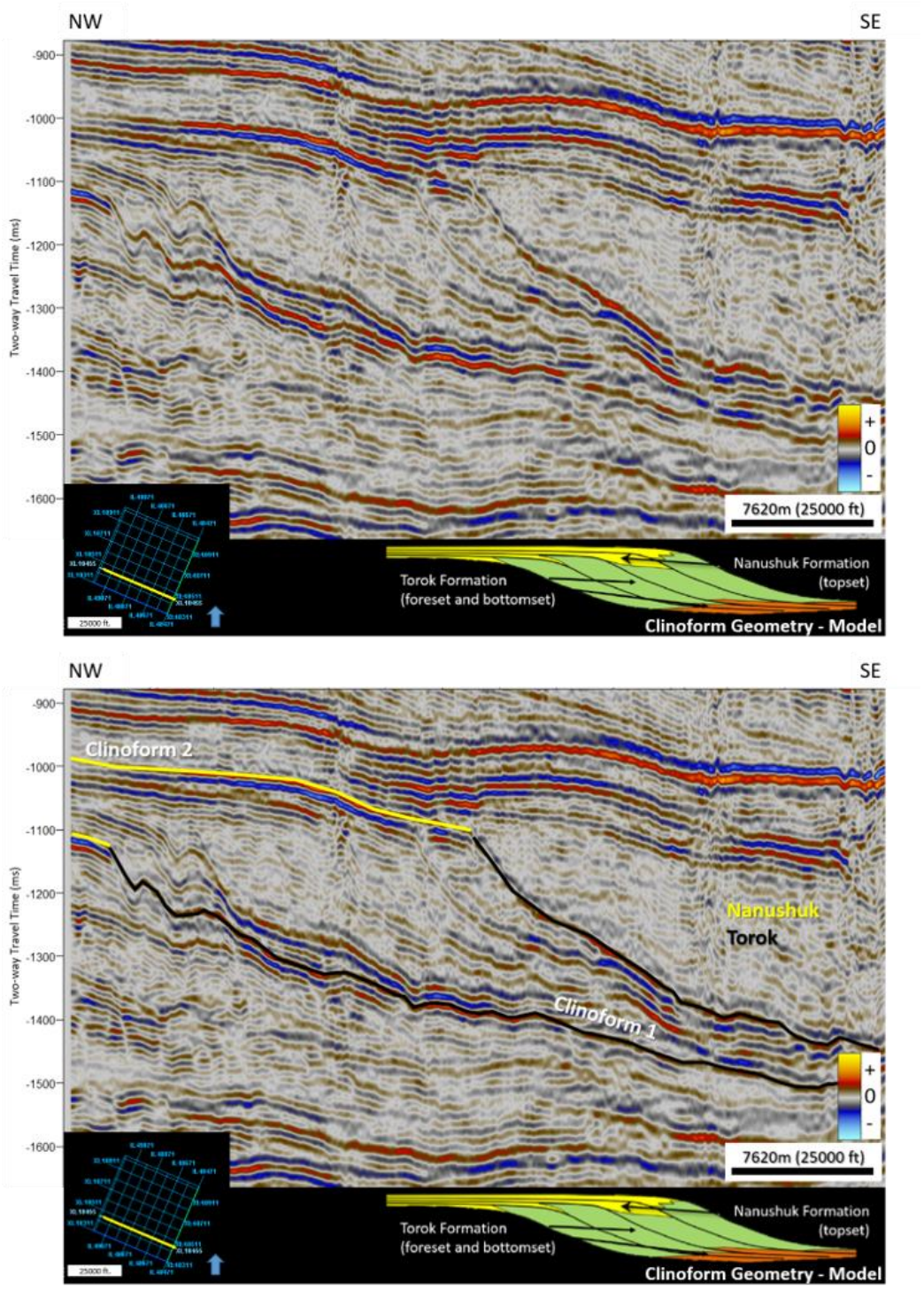

Figure 5.2 Arbitrary seismic line from the Nanuq South 3D survey. This NW-SE line through the Nanuq South 3D seismic survey illustrates two examples of clinoform surfaces mapped throughout the survey area. Each clinoform surface includes the time-correlative Nanushuk and Torok formations.

yield geologically meaningful results. The results of the extraction of seismic attributes indicated the presence of geologically relevant amplitude anomalies. These anomalies potentially correspond to shelf-edge delta deposits or other clay-poor potential reservoir material from local shelf, slope, and basin floor depositional environments.

The RMS and sweetness seismic attributes extracted from the Nanuq South 3D post-stack seismic volume were draped over each of the interpreted surfaces to aid in the detection of geologically relevant amplitude anomalies. This visualization technique indicated the presence of a relatively clay-poor material potentially corresponding to perched shelf edge deltas, shoreface sands, slope apron deposits, turbidite deposits, or basin floor fan deposits (Figure 5.3). This detection of the relative clay content via seismic interpretation and seismic amplitude extraction was successfully used as a first step in discovering and deliniating potentially prolific conventional hydrocarbon reservoirs.

5.2 Petrophysical Interpretation and Multi-Mineralogical Modeling [PowerLog^{TM}]

5.2.1 Well Correlation and Petrophysical Analysis

Prior to performing the petrophysical analysis, the adjusted AOGCC formation tops were used as a starting off point for the well log correlation process and subsequently edited as needed to reflect the true stratigraphy of the basin (Figure 5.5). For penetrations of the Nanushuk Formation, individual sand zones were also picked in each well, allowing for the properties within individual parasequences to be readily analyzed and manipulated. The log signature of the Nanushuk Formation as measured by the gamma ray log is an easily recognizable, coarsening upward, funnel shaped response typical of prograding sedimentary features.

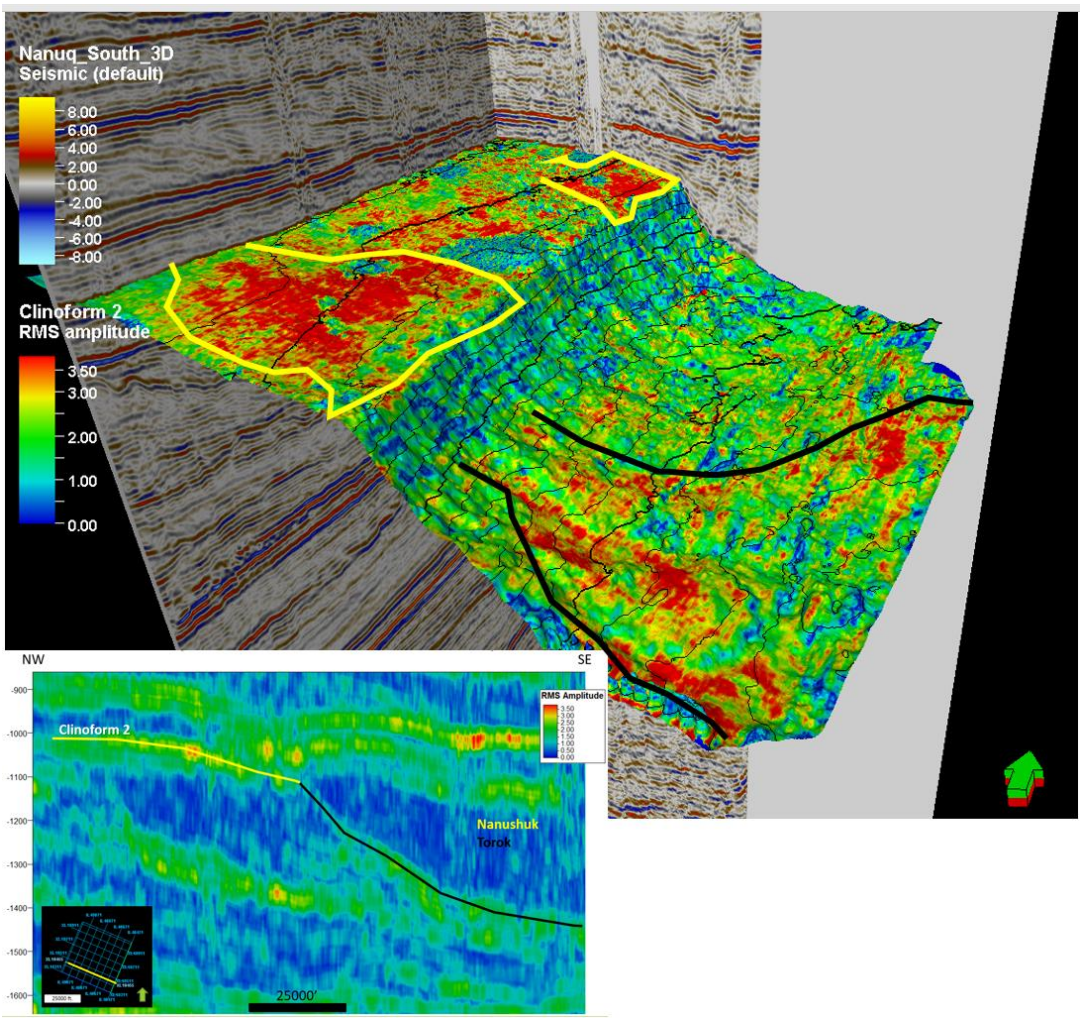

Figure 5.3 RMS amplitude attribute draped on an interpreted surface. (Top) High RMS amplitude anomalies enclosed by a solid yellow line denotes potential shelf edge deposits within the topset facies demarking potential clay-poor Nanushuk reservoirs. High RMS amplitude anomalies enclosed by a solid black line denotes potential slope apron deposits and basin floor fan deposits within the foreset and bottomset facies, demarking possible clay-poor Torok reservoirs. (Bottom) Cross line through the RMS Amplitude volume showing areas with high RMS anomalies (red areas) along the paleo-shelf as marked by the yellow Nanushuk horizon.

A robust petrophysical analysis was performed in CGG'S PowerLog™ software package for each well in the study area using standard petrophysical equations and cross-plot analyses: calculation of density-based porosity in a corrected background matrix, neutron matrix conversion, calculation of average porosity, calculation of clay volume, Pickett plot analysis, and calculation of water saturation (Tables 4.1, 4.2, and 4.3). In addition, wells with available dipole sonic logs were used to calculate the P-wave velocity (V_p), S-wave velocity (V_s), and the V_P/V_S ratio. The V_P/V_S ratio is sensitive to critical rock properties, including impedance, porosity, fluid saturation, and rock type.

Geophysical well logs are a continuous record of measured or induced rock properties as penetrated by the borehole path (Rider and Kennedy, 2011). Even boreholes with problematic data sets impacted by less than ideal borehole conditions can still provide impactful information through the application of petrophysical relationships and statistical modeling (Moss and Harrison, 1985). In instances where key measured or induced geophysical logs were missing or of unusable quality, data from other tools can be used to approximate the property. The Itkillik River Unit 1 log package includes the key logs required for seismic inversion – log-measured density and sonic data; however, the density log was missing approximately 2000' of data from the Torok section, possibly due to a stuck tool during the logging run. To generate the missing data, Gardner's equation (Equation 5.1) was applied to approximate the density (ρ) using P-wave velocity (Vp).

$$\rho = \propto V_p{}^{\beta} \quad \text{(Equation 5.1)}$$

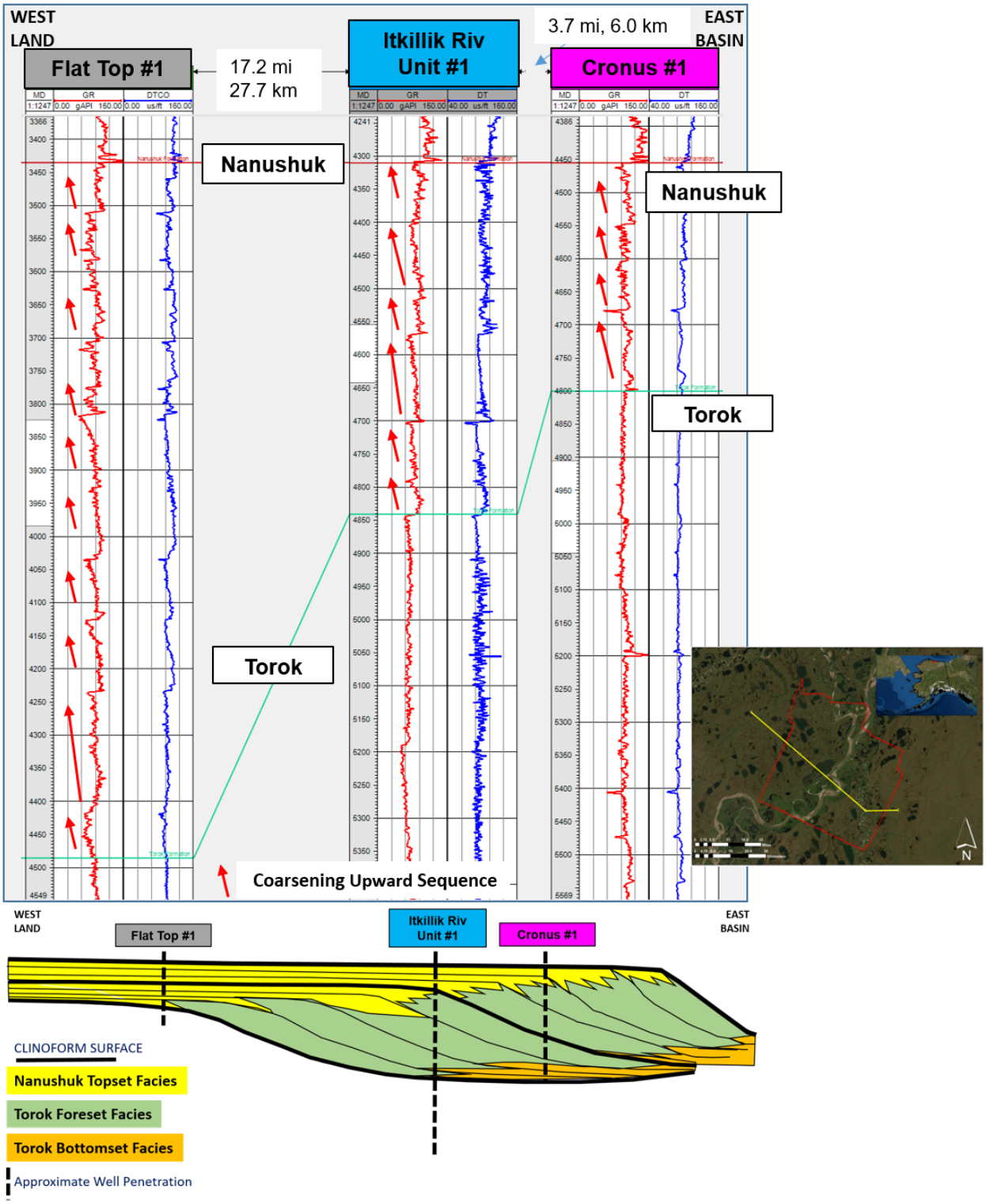

Figure 5.4 West to east well cross-section. This cross-section was flattened on the top Nanushuk horizon. The red curve in track one of each well display is the gamma ray

(GR) curve. The gamma curve over the Nanushuk interval in all three wells demonstrates the typical coarsening upwards gamma log signature of the Nanushuk formation. This figure also depicts a generalized clinoform below the log cross section, illustrating the relative locations of the well penetrations in reference to the clinoform surfaces and in reference to the spatial distribution of the seismic facies within the clinothem package. The landward Flat Top 1 well penetrates a thicker section of Nanushuk topset facies, while the basinward Cronus 1 well penetrates a thicker section of Torok bottomset facies. The centralized location of the Itkillik River Unit 1 well penetrates all three Brookian facies: Nanushuk topset facies and Torok foreset and bottomset facies.

The computed or transformed Gardner's density curve was spliced into the original density curve over the interval of bad data to generate a continuous density curve within the Itkillik River Unit 1 penetration of the Torok Formation (Figure 5.5).

Water saturations were calculated using two different empirical relationships and compared against core data for validation (Equations 5.2 and 5.3).

$$S_W\ (Archie) = \left[\frac{a\ R_W}{\varphi^m (R_t)}\right]^{\frac{1}{n}} \text{ (Equation 5.2)}$$

$$\frac{1}{R_t} = \frac{\varphi^m {S_w}^n}{aR_w} + \frac{V_{SH} S_W}{R_{SH}} \text{ (Equation 5.3)}$$

For Equations 5.2 and 5.3, phi (φ) is the porosity from an inserted log, R_t is true formation resistivity from an inserted log, and V_{shale} is computed shale volume from an inserted log. The remaining variables (a, m, n, R_{sh} and R_w) are constants which were selected at each well location based on visual inspection of the available data. Archie's constants (a, m, and n) were determined graphically from Pickett Plot analysis over the reservoir interval by adjusting the values for a, m, and n until the plotted porosity, resistivity pairs were plotted at or above the 100% water saturation line and such that points likely corresponding to a hydrocarbon accumulation plotted at or above the 50% water saturation line. As an example, the final values dervived using Pickett Plot analysis for the Horseshoe 1 well are displayed in Table 5.1 and Figure 5.6.

Constant	abbrev.	value*
Water Resistivity	R_w	0.3
Tortuosity Factor	a	1
Cementation Factor	m	1.8
Saturation exponent	n	2
*derived from Pickett Plot analysis		

Table 5.1 Horseshoe 1 Archie's Constants

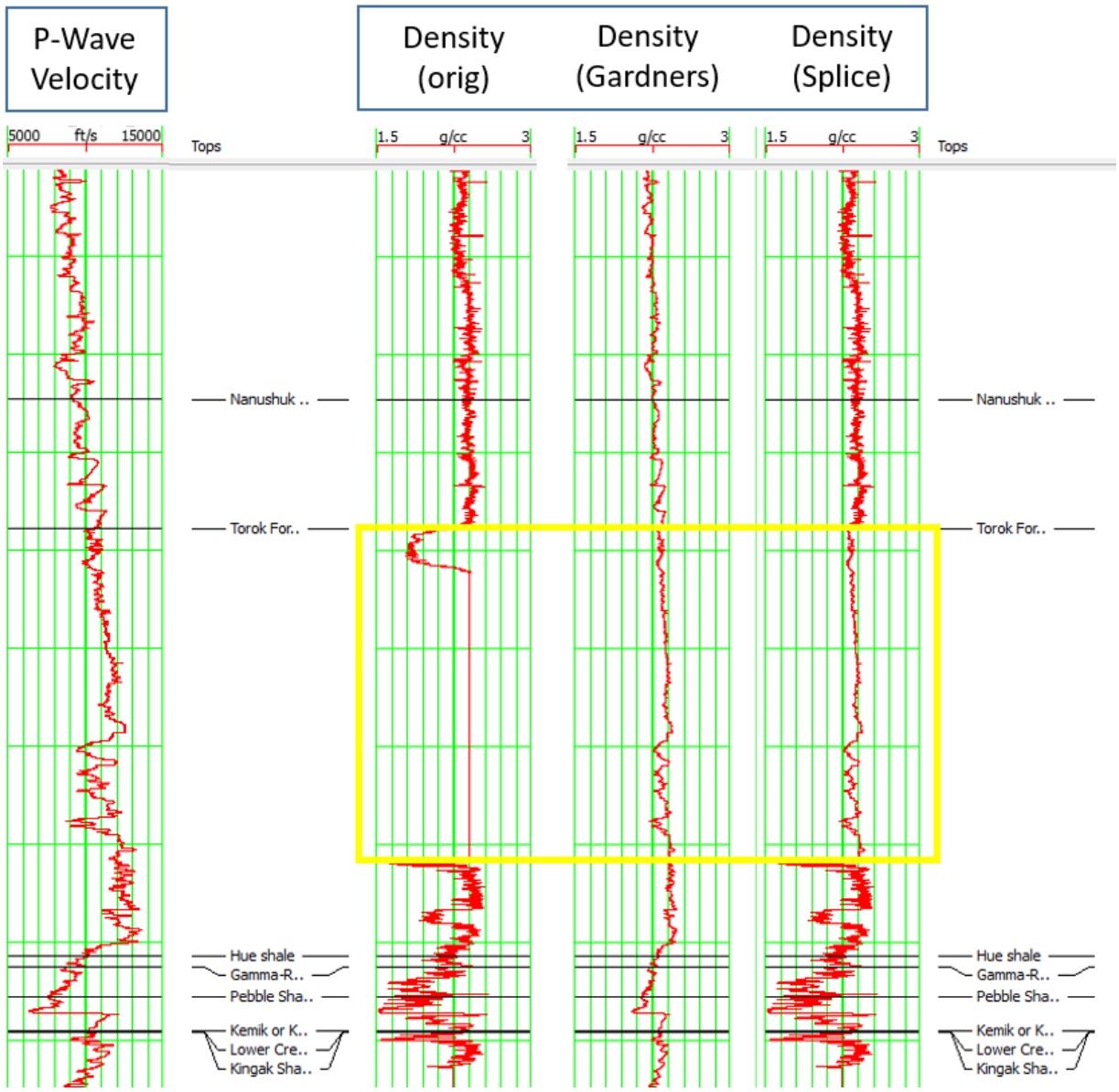

Figure 5.5 Density splicing example from Itkillik River Unit 1 using Gardner's equation to generate data in the missing section (yellow box, "Density (orig)). The P-wave velocity curve (far left track) was used in Gardner's equation (Equation 5.1) to yield Gardner's density (right side, middle track). This calculated curve replaced the missing/problematic data in the original curve, yielding the spliced Density curve (right side, far right track).

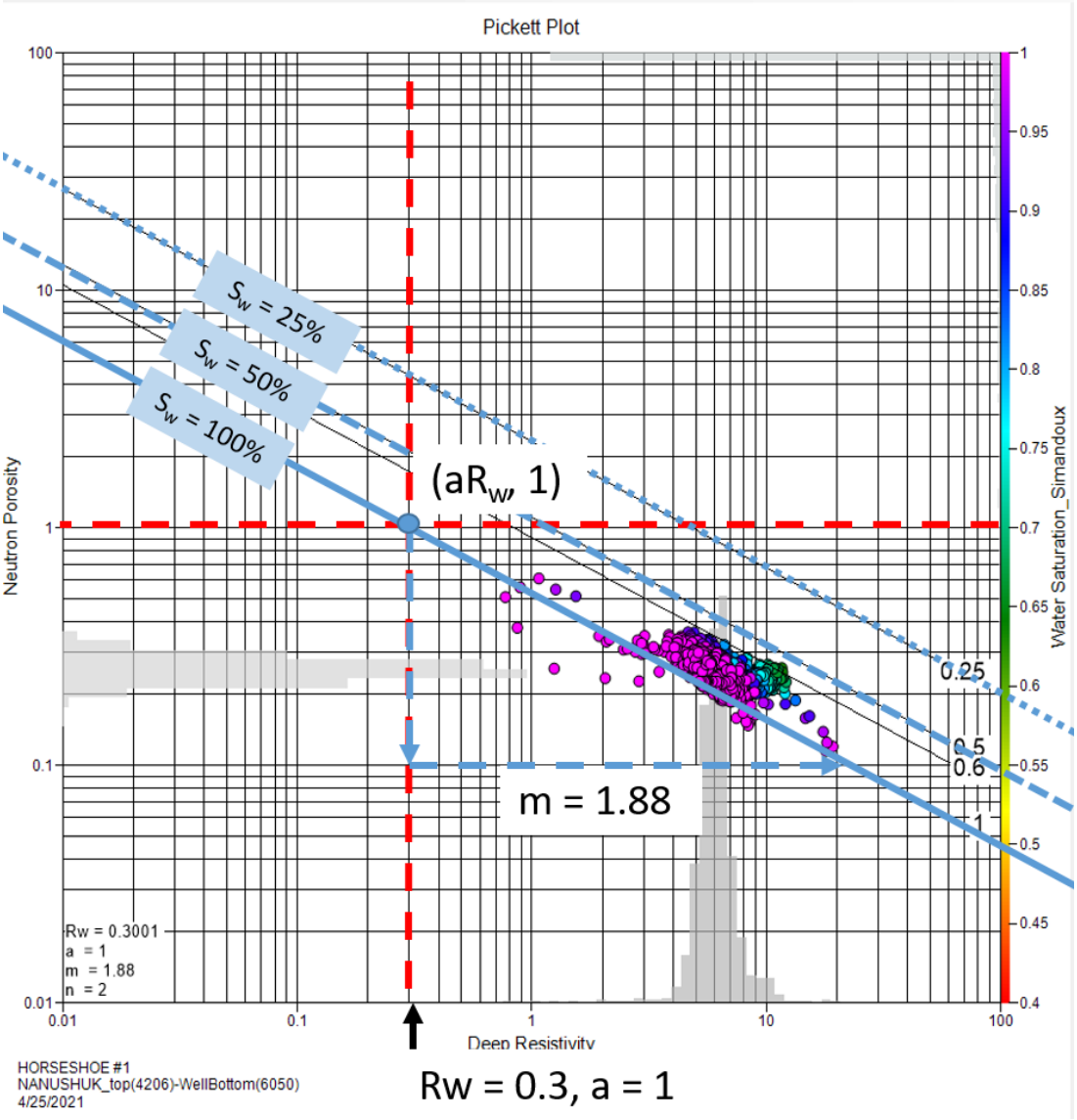

Figure 5.6 Horseshoe 1 Pickett plot. Deep resistivity is plotted on the x-axis, neutron porosity on the y-axis, and the data is colored using water saturation values. The 100% water saturation line (solid blue), 50% water saturation line (long dashed blue), and 25% water saturation line (short dashed blue) are plotted on the log-log plot. The slope of this line is controlled by the cementation factor (m), which for clay-rich reservoirs fluctuates between 1.87 and 1.89 (Crain, 2009).

The remaining constant (R_{sh}) was estimated by visually examining the resistivity log in a shale zone with a high gamma ray response and noting the resistivity log value in that zone.

The resulting log data from solving Archie's equation (Equation 5.2) using the Pickett plot derived Archie's constants did not provide a good match to core measured saturations. The results of using the same Pickett plot derived Archie's constants as inputs into the Simandoux equation (Equation 5.3) provided a much better match to core measured saturations (Figure 5.7). The Simandoux equation takes into account the resistivity based clay-effect, and as such, generated a water saturation curve that better matched the measured core data (Bhattacharya and Verma, 2020). Comparing Simandoux's water saturation with core-measured water saturation yielded up to a 5-10% error when comparing individual, overlapping points of the two data sets.

5.2.2 Multi-Mineralogical Modeling

These derived petrophysical properties were used in the the StatMin™ module within CGG'S PowerLog™ software package to generate a multi-mineralogical model. The model outputs volumetric proportions of sand, clay, water, and hydrocarbons. This multi-mineralogical modeling was performed for six of the seven wells in the study area, and the models were iterated a 10-15 times to reduce error. The model generated reconstructed versions of each input log, and the model was adjusted and improved until the reconstructed curves matched the input curves as best as possible. For each multi-mineralogical model, five input curves were used to generate four modeled properties. This ratio of N:(N-1), where N is the number of input logs, is ideal to ensure the model is balanced (Moss and Harrison, 1980).

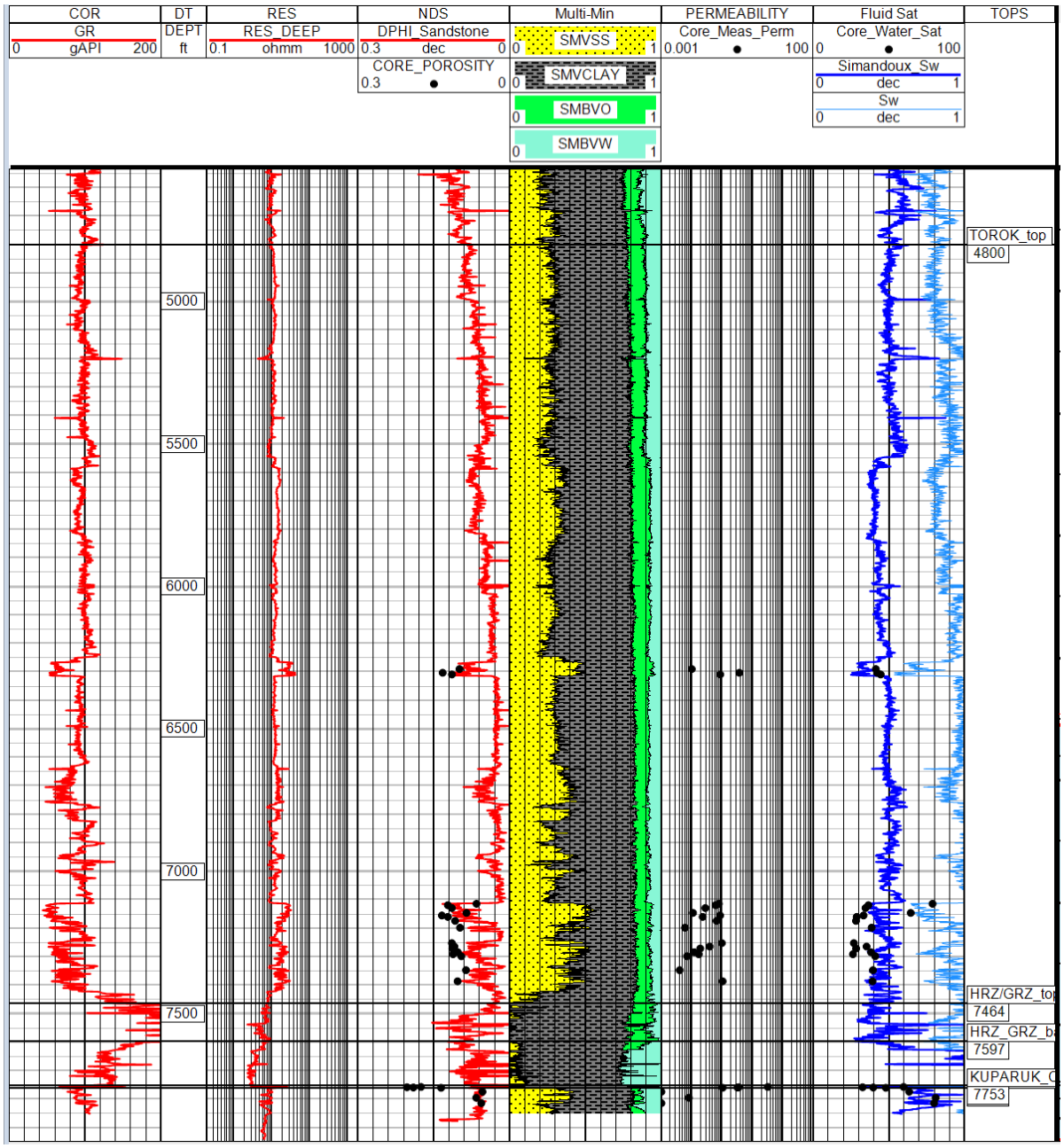

Figure 5.7 Horseshoe 1 well log display. Track 6, “Fluid Sat” contains two computed water saturation curves. The dark blue curve was calculated using the Simandoux equation, while the light blue curve was calculated using the Archie equation. Black circles indicate core porosity measurements. The Simandoux water saturation curve provides a better visual match with the core data as compared to the light blue curve.

Statistical modeling utilizes common geophysical logs, computed parameters including formation water resistivity, shale resistivity, formation temperature, and water salinity, and core data to generate multi-mineralogical models estimating mineralogy and pore fluid in the borehole. Performed correctly, these results are meant to mimic data from expensive downhole spectroscopy tools. Multi-mineralogical modeling results were compared to a measured elemental analysis log (Elemental Capture Spectroscopy) in the Horseshoe 1A well for validation. The results of the statistical model were a good visual match when compared to the measured spectroscopy data at the Horseshoe 1 well location. The largest discrepancy between the modeled results and the measured results from the spectroscopy was due to the model not solving for limestone. This discrepancy could be remedied by adding limestone as a mineral solution and modeling for this additional lithology.

As a last step, the reconstructed porosity curve was compared to core measured porosity data. This visual inspection indicates a moderately good fit to the measured core data. The maximum difference between core-measured porosity and the reconstructed porosity log was up to a 15% difference in porosity, which is substantial, but the average error was reduced to a more reasonable 3-5% porosity difference between datasets in the cored interval.

5.2.3 Petrophysical Cross-plots

A series of petrophysical cross-plots were generated using CGG'S PowerLog™ software package for each well in the study. Each cross-plot reveals important information about how changes in lithology, pore fluid content, and porosity impact the petrophysical response experienced at each well location. Using the Horseshoe 1 well

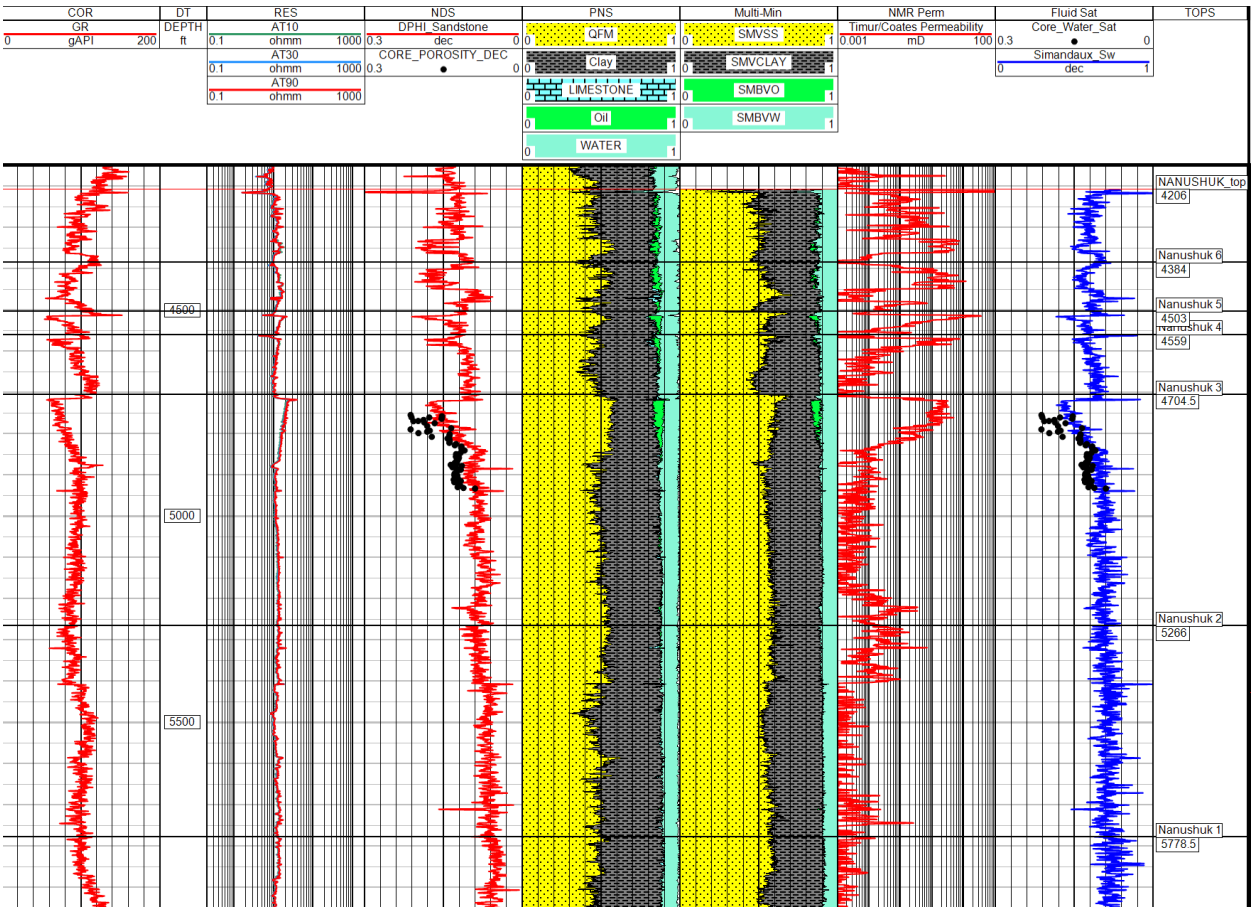

Figure 5.8 StatMin™ display: Horseshoe 1. Tracks 4 and 5, labeled “PNS” for Pulsed Neutron Spectroscopy and “Multi-Min” for Multi-mineralogical Modeling contain measured (Track 4) and modeled (Track 5) fluid and mineral volumes for the Horseshoe 1 well. The modeled results fit the measured results at this well location upon visual inspection. The reconstructed porosity curve (red) in the third track (labeled NDS) was co-plotted with porosity measurements from core samples (black dots). While some individual points exhibit a substantial error (+15% porosity difference), the reconstructed curve was within 3-5% of the core measured porosity values across the cored interval.

as an example, the following petrophysical cross-plots were generated for analysis: neutron porosity versus (vs.) density, acoustic impedance vs. porosity, density vs. porosity, P-wave velocity vs. porosity, and acoustic impedance vs. water saturation.

The neutron porosity vs. density cross-plot over the Nanushuk interval in the Horseshoe 1 well indicates a relatively high clay content associated with data from zones that are more sand-dominant (Figure 5.9). The acoustic impedance vs. porosity cross-plot reveals the typical inverse relationship between these two log properties (Figure 5.10). Data points exhbiting high porosity values have corresponding low acoustic impedance values. The regression equation relating log computed impedance to core calibrated porosity was used to transform the seismic inversion volume to the porosity volume. The density vs. porosity cross-plot illustrates inverse relationship between porosity and density, where high porosity corresponds to low density and vice-versa (Figure 5.11). This density vs. porosity cross-plot can also be used as a quality control check to visually inspect for the presence of the inverse relationship and identify areas with “bad” density data (data that plots “off” the charts). The P-wave velocity vs. porosity cross-plot also illustrates the expected inverse relationship between these properties, with high porosity values corresponding to low velocity values (Figure 5.12). The acoustic impedance vs. water saturation cross-plot for this well exhibits two separate trends in the data based on relative clay volume (Figure 5.13). The P-wave impedance vs water saturation cross-plot was manipulated further using sample highlighting to illuminate the points on the log display with low water saturation and low fractional shale (clay) volume (Figure 5.14).

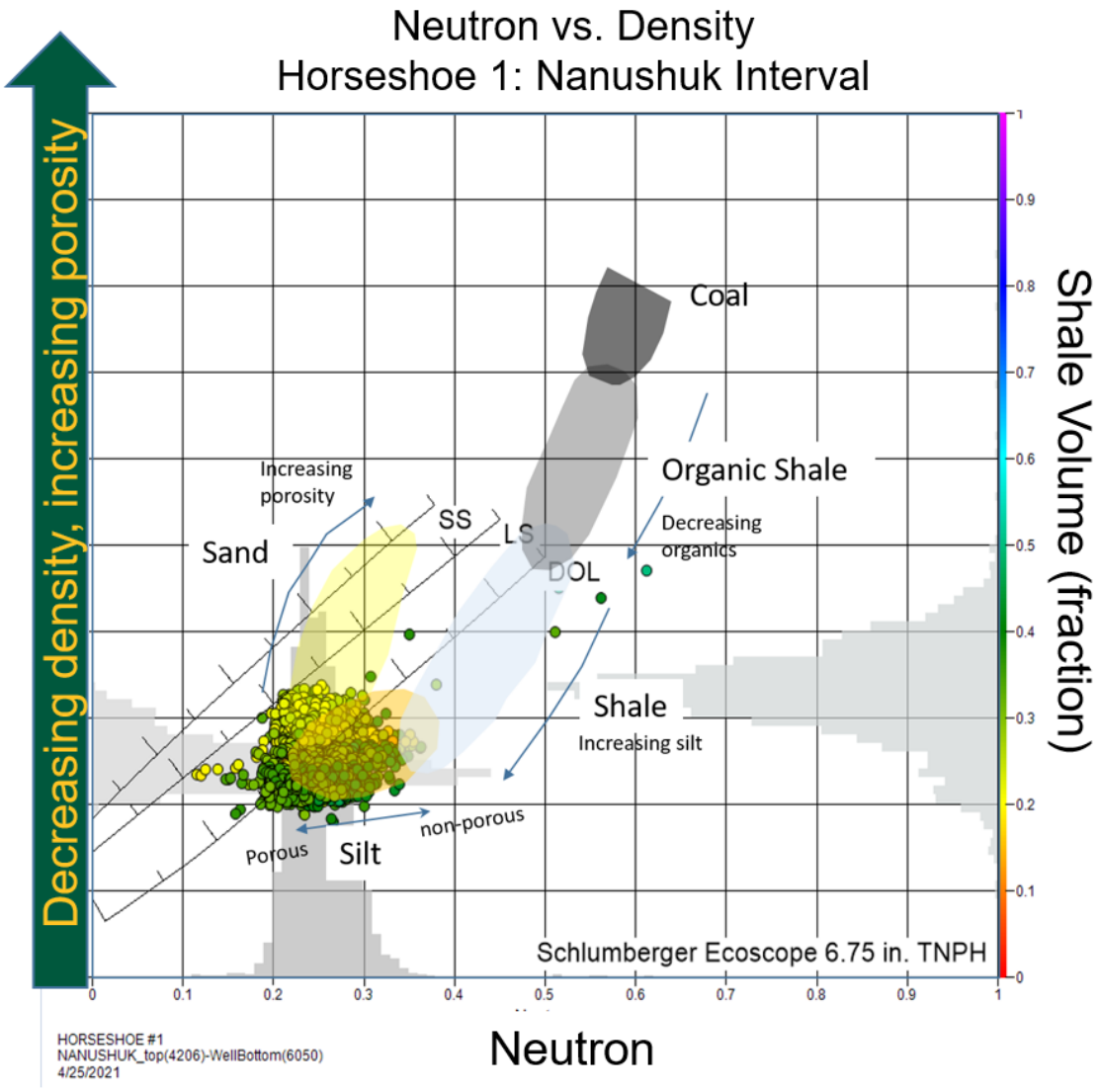

Figure 5.9 Neutron porosity vs density cross-plot: Horseshoe 1 – Nanushuk interval. This cross-plot has an overlay indicating the typical zones for these lithologies. The data from the Nanushuk interval in the Horseshoe 1 well indicates a silty lithology based on visual inspection of this cross-plot. This cross-plot based interpretation is confirmed by the portion of the well's geologic report detailing the mudlogger's notes (Narbors, 2017).

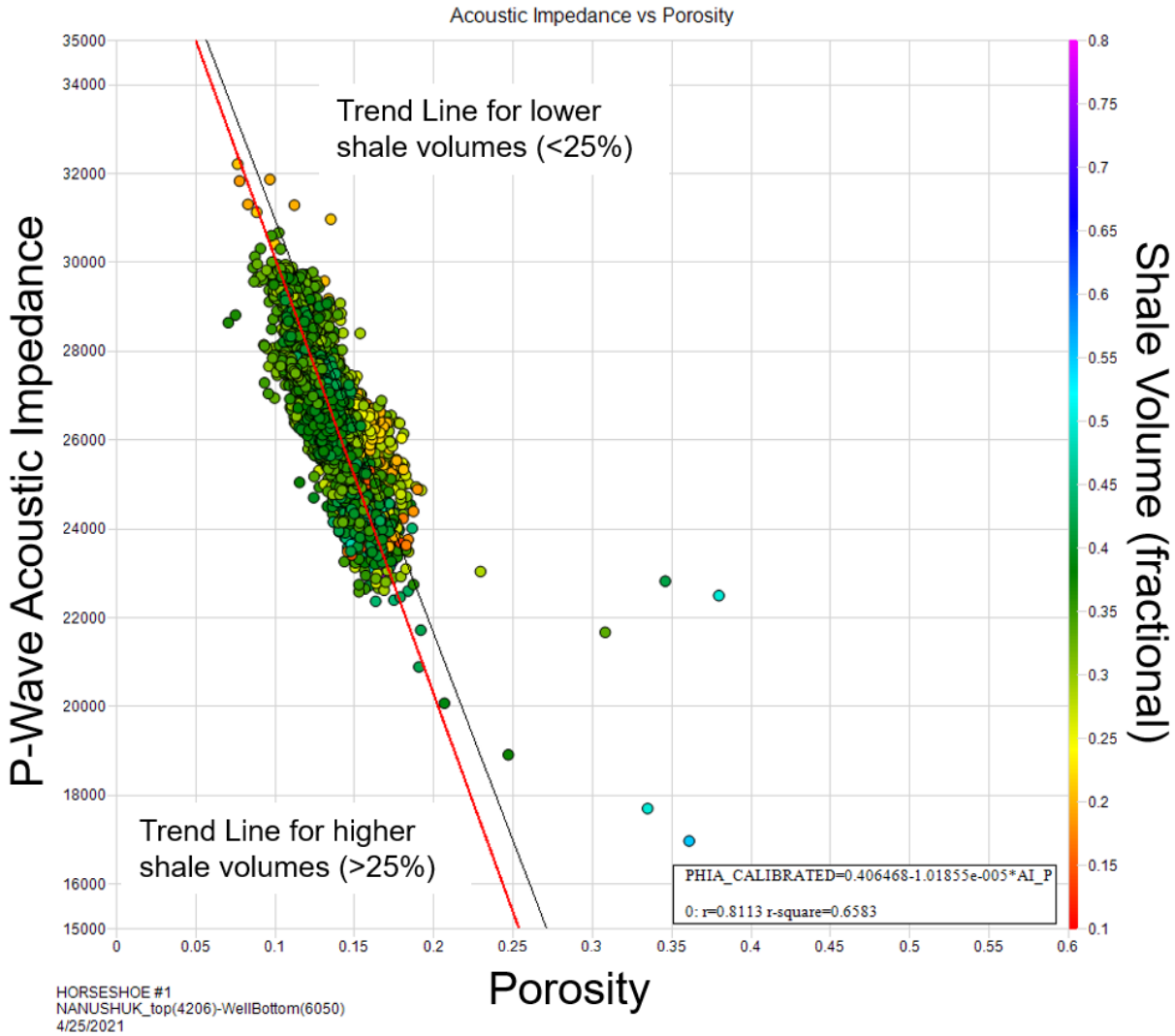

Figure 5.10 Acoustic impedance vs. porosity cross-plot: Horseshoe 1 – Nanushuk interval. This cross-plot contains porosity values plotted along the x-axis, and P-wave acoustic impedance values across the y-axis, colored by fractional shale volume. The cross-plot reveals an inverse relationship between porosity and impedance, with high porosity values corresponding to low acoustic impedance values.

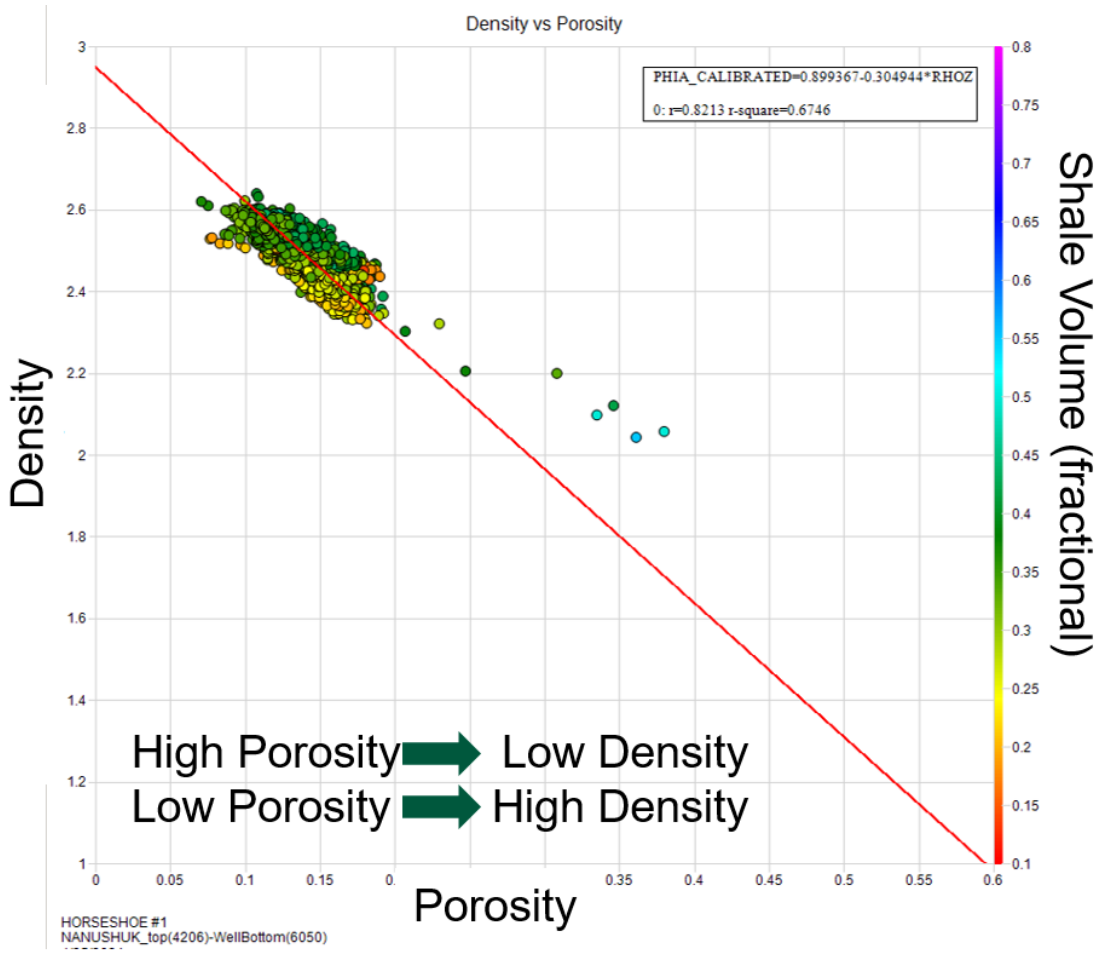

Figure 5.11 Density vs. porosity cross-plot: Horseshoe 1 – Nanushuk interval. This cross-plot contains porosity values plotted along the x-axis, density values along the y-axis and is colored by fractional shale (clay) volume. This cross-plot reveals the inverse relationship between porosity and density, with high values of porosity corresponding to low values of density.

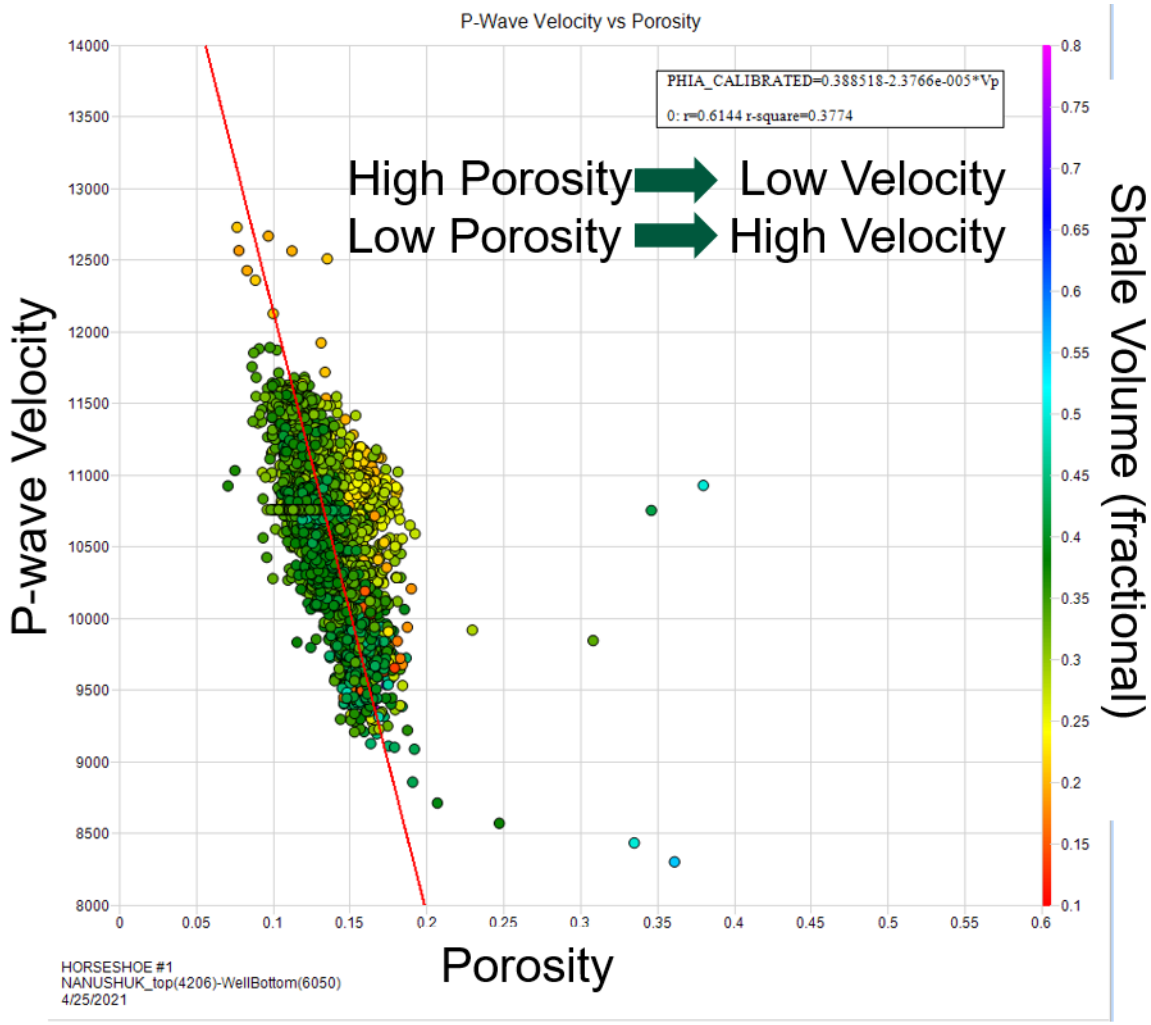

Figure 5.12 P-wave velocity vs. porosity cross-plot: Horseshoe 1 – Nanushuk interval. Porosity is plotted along the x-axis, P-wave velocity is plotted along the y-axis, and the data is colored by fractional shale (clay) volume. The cross-plot reveals the inverse relationship between porosity and P-wave velocity, with high porosity values corresponding with low velocity values.

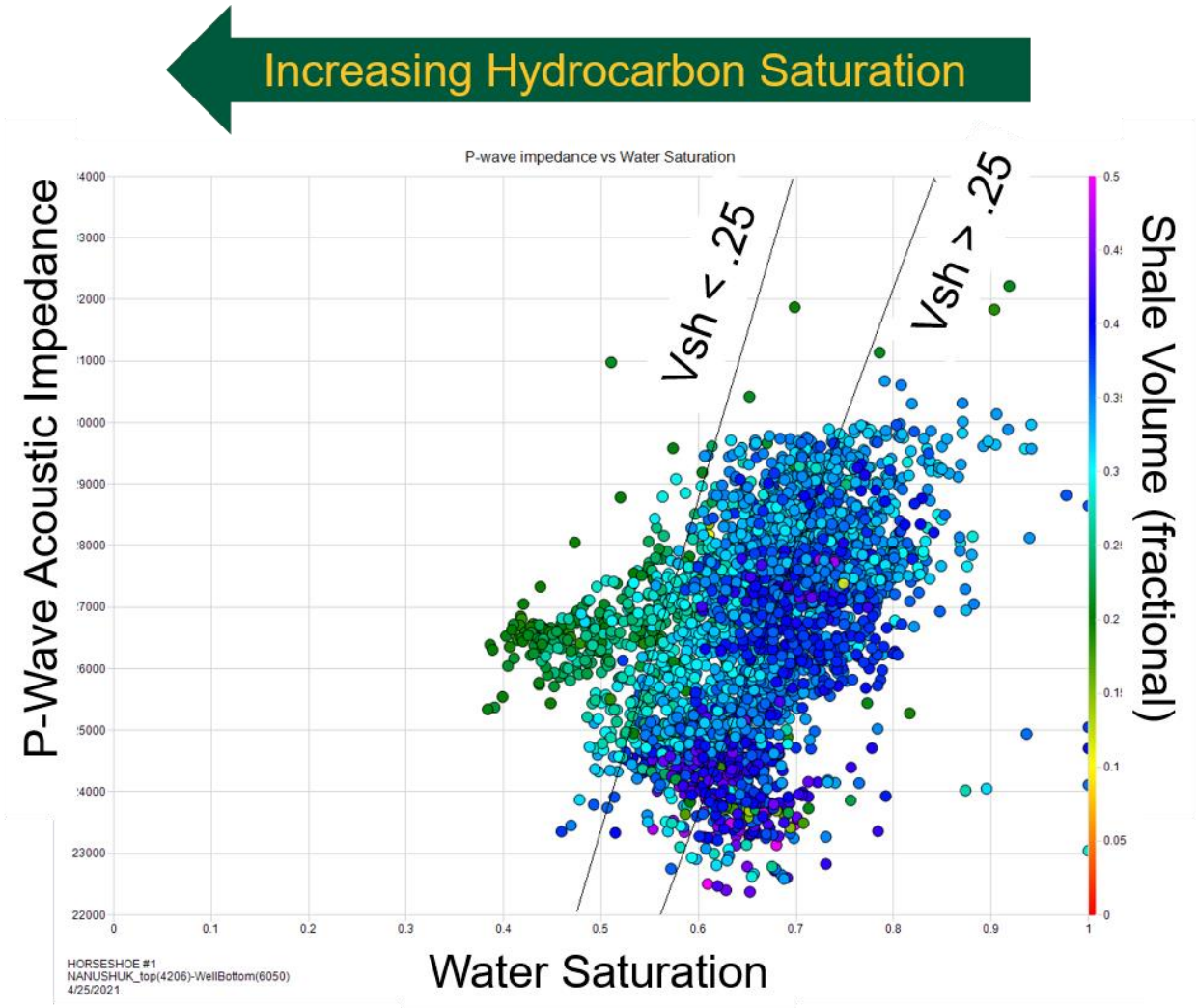

Figure 5.13 P-wave acoustic impedance vs. water saturation cross-plot: Horseshoe 1 – Nanushuk interval. Water saturation is plotted along the x-axis, P-wave acoustic impedance along the y-axis, and the data is colored by fractional shale (clay) volume. Two regression lines were plotted by introducing a data discriminator, limiting the data set based on the volume of shale (values of V_{sh} > .25 separated from values of V_{sh} < .25)

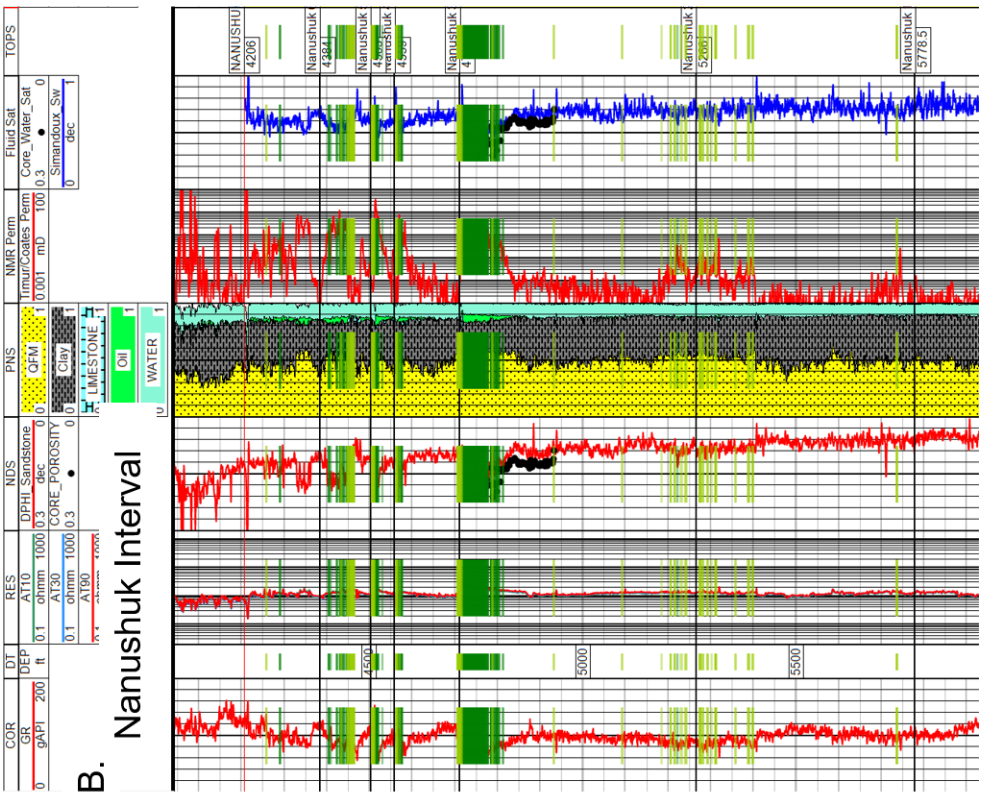
B.
Nanushuk Interval
COR
GR
gAPI
DT
DEP
ft
RES
AT10
AT30
AT80
ohmm
NDS
DPHI_Sandstone
CORE_POROSITY
dec
PHS
QFM
Clay
LIMESTONE
Oil
WATER
NMR Perm
Timur/Coates Perm
mD
Fluid Sat
Core_Water_Sat
Simandoux_Sw
TOPS
NANUSHU
Nanushuk
4206
5778.5
4500
5000
5500

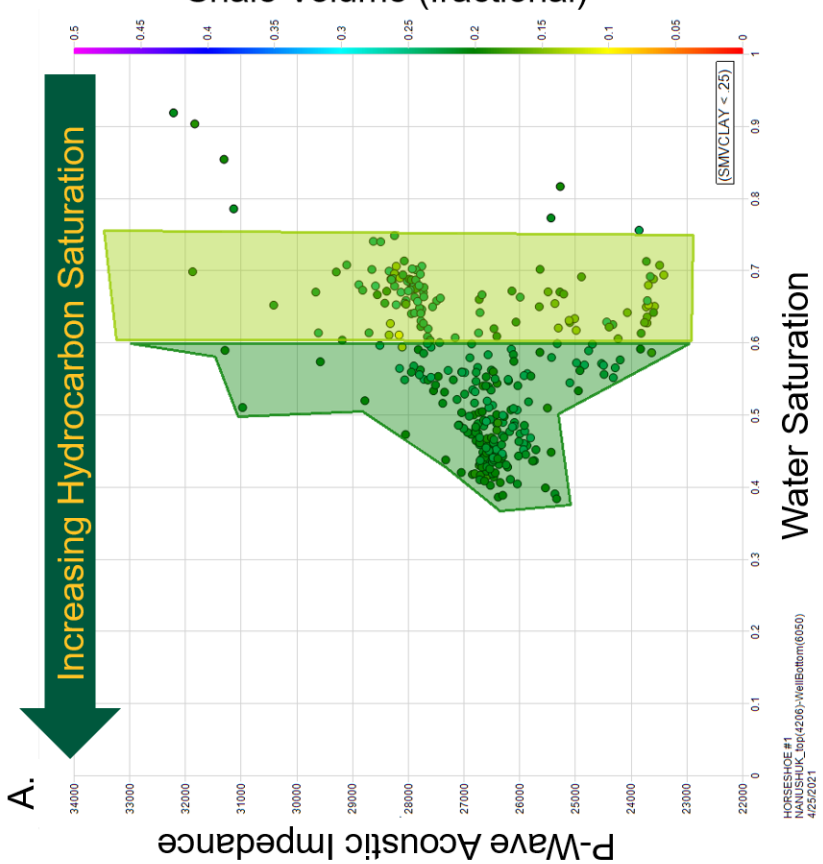
A.
Increasing Hydrocarbon Saturation
P-Wave Acoustic Impedance
Water Saturation
Shale Volume (fractional)
(SMVCLAY < .25)
HORSESHOE #1
NANUSHUK_top(4206)-WellBottom(6050)
4/25/2021

Figure 5.14 Sample highlighting using a shale volume discriminator: Horseshoe 1 – Nanushuk interval.

A. This cross-plot is the same range of data displayed in Figure 5.13, but with an added discriminator allowing only the points where V_{sh} is less than 25% to plot on the graph. These clay-poor data points were then segregated into two groups, the dark green group containing points with < .6 (60%) water saturation, and the light green group containing points with between .6 and .75 (60% - 75%) water saturation.

B. Linked well log display showing the corresponding dark green and light green sample sets. The dark green samples correlated perfectly with the main target oil reservoir of the Horseshoe 1 well.

5.3 Post-Stack Seismic Inversion [HampsonRussell^{TM}]

5.3.1 The Forward Model

Once the basic seismic interpretation and the petrophysical analysis was completed, a more robust well to seismic study was performed using the HampsonRussell^{TM} “Wells” module on each well in the study area. This process, known as forward seismic modeling, generates a synthetic seismogram that models what a seismic trace should look like based on the log measured impedance data (Figure 5.15) (Russell, 2017).

The forward seismic modeling process used acoustic impedance (the product of the log based sonic velocity and density) to generate a reflection coefficient log. The reflection coefficient log was then convolved with a statistical wavelet extracted from the original seismic trace data, generating a synthetic or modeled trace along the borehole. This synthetic trace was then compared to the actual seismic trace data extracted along the borehole. Peaks and troughs from the extracted seismic trace were correlated with the synthetic trace data by stretching or squeezing the synthetic trace to match the reflectors of original trace data. This stretching and squeezing process calibrated the log-measured velocity data to the seismic velocity data. The log correlation process was tested using a variety of wavelets extracted at multiple well locations until a best-fit model was achieved with minimal error between the actual seismic trace and the modeled result. Ultimately, a statistical wavelet extracted from the full offset survey within a limited time window (950-1550 ms) was chosen for the initial log correlation (Figure 5.16).

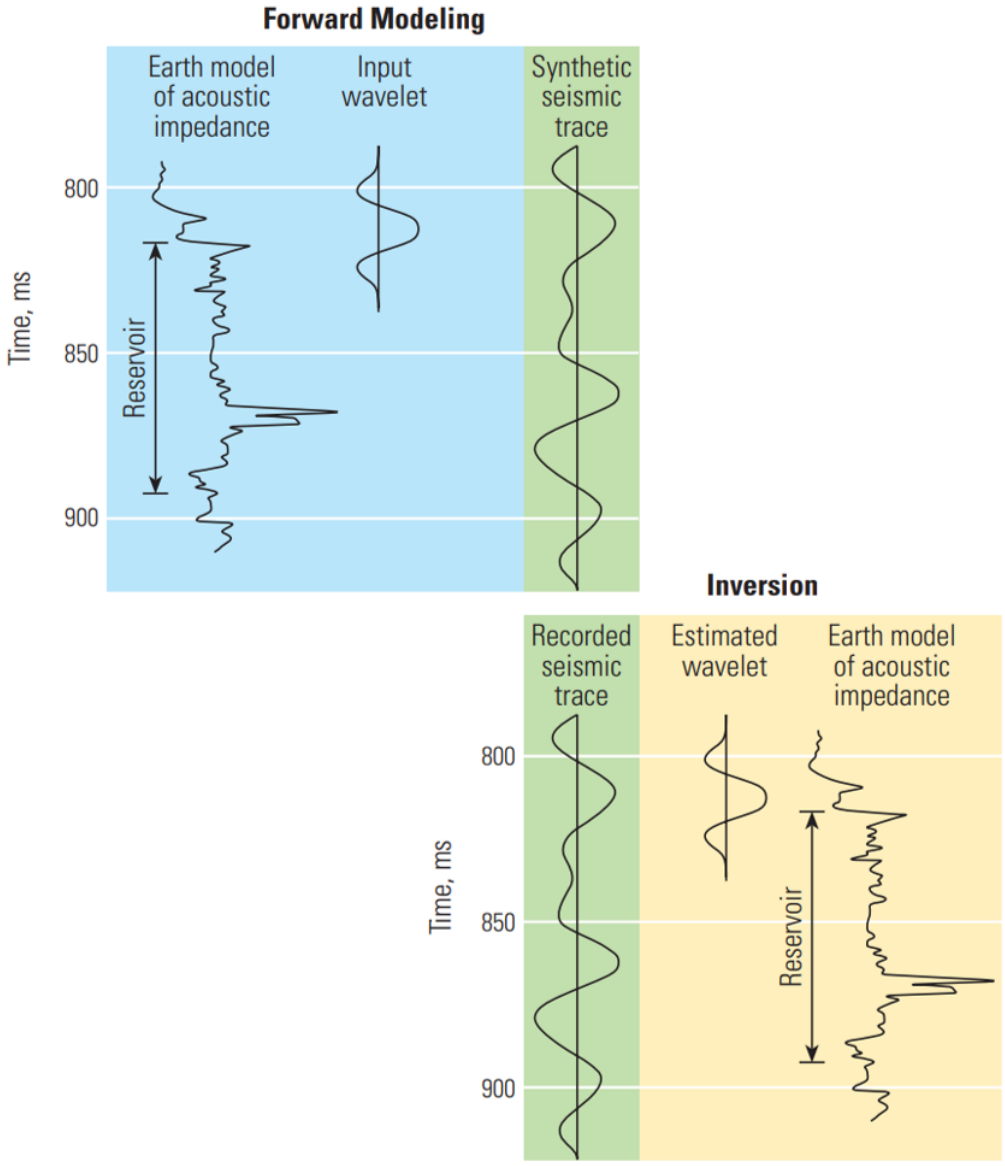

Figure 5.15 Forward and inverse modeling (Russell, 2017). This figure illustrates the forward and inverse modeling process. The forward model uses well calculated acoustic impedance convolved with an extracted wavelet to generate a synthetic (modeled) seismic trace. Inversely, the inverse model uses the recorded seismic trace and removes the wavelet effect from the data, generating a modeled inverted impedance curve.

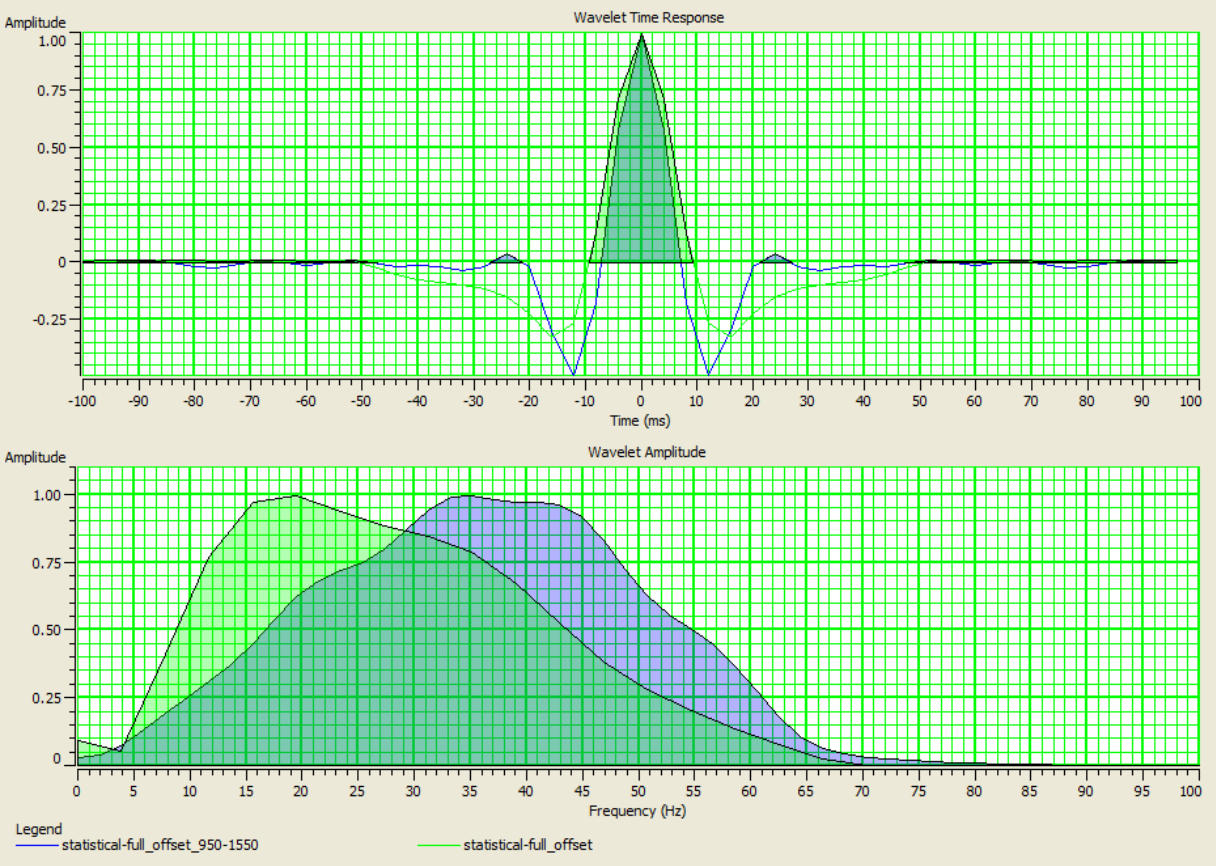

Figure 5.16 Wavelet extraction - Nanuq South 3D seismic volume. The wavelet shown in blue is the statistical Ricker wavelet, extracted from the full offset data over a time window from 950 – 1550ms. The wavelet shown in green is the statistical Ricker wavelet extracted from the full time range of the Nanuq South 3D data set. Ultimately, the blue wavelet with the limited time window was the final selection for committing log correlation across all area wells in the initial phase of the well correlation process. This choice was made because the limited window allows the wavelet to only retain relevant frequency data (the difference in frequency content is shown along the lower graph).

A precise seismic-well tie is crucial for the inversion, so this log correlation process was performed on all study wells. The finalized stage one forward modeling results are shown for the Itkillik River Unit 1 well in Figure 5.17. The correlation window was limited to the window of interest, and an acceptable well tie was achieved (correlation value of .716, a perfect match is a correlation value of 1).

Once the initial synthetic tie was established for all of the project wells, the correlation process was repeated using a full phase wavelet extracted at the well location for each well in the study area (Figure 5.18). This process, though time consuming, successfully raised the correlation in all study wells from a 0.61 minimum correlation value to a 0.98 minimum correlation value. The second stage log correlation results are shown for the Itkillik River Unit 1 well in Figure 5.19.

Once all of the wells were properly correlated, a low frequency geologic background model was created. This model will guide the seismic inversion process and provide the low frequency component which is otherwise missing from the seismic data. For the purposes of this study, only the Itkillik River Unit 1 well was used to train the model. The only other inputs to the background model are a wavelet, the original trace volume, and regionally interpreted geologic horizons. The final result from the forward modeling process was a low frequency geologic background model generated using a forward seismic modeling process based on data from a single legacy well (Itkillik River Unit 1) (Figure 5.20). A small degree of horizon smoothing and extension performed on the horizon data to ensure there were no gaps or large peaks in the surfaces, as these situations generate unwanted effects in the inverted data.

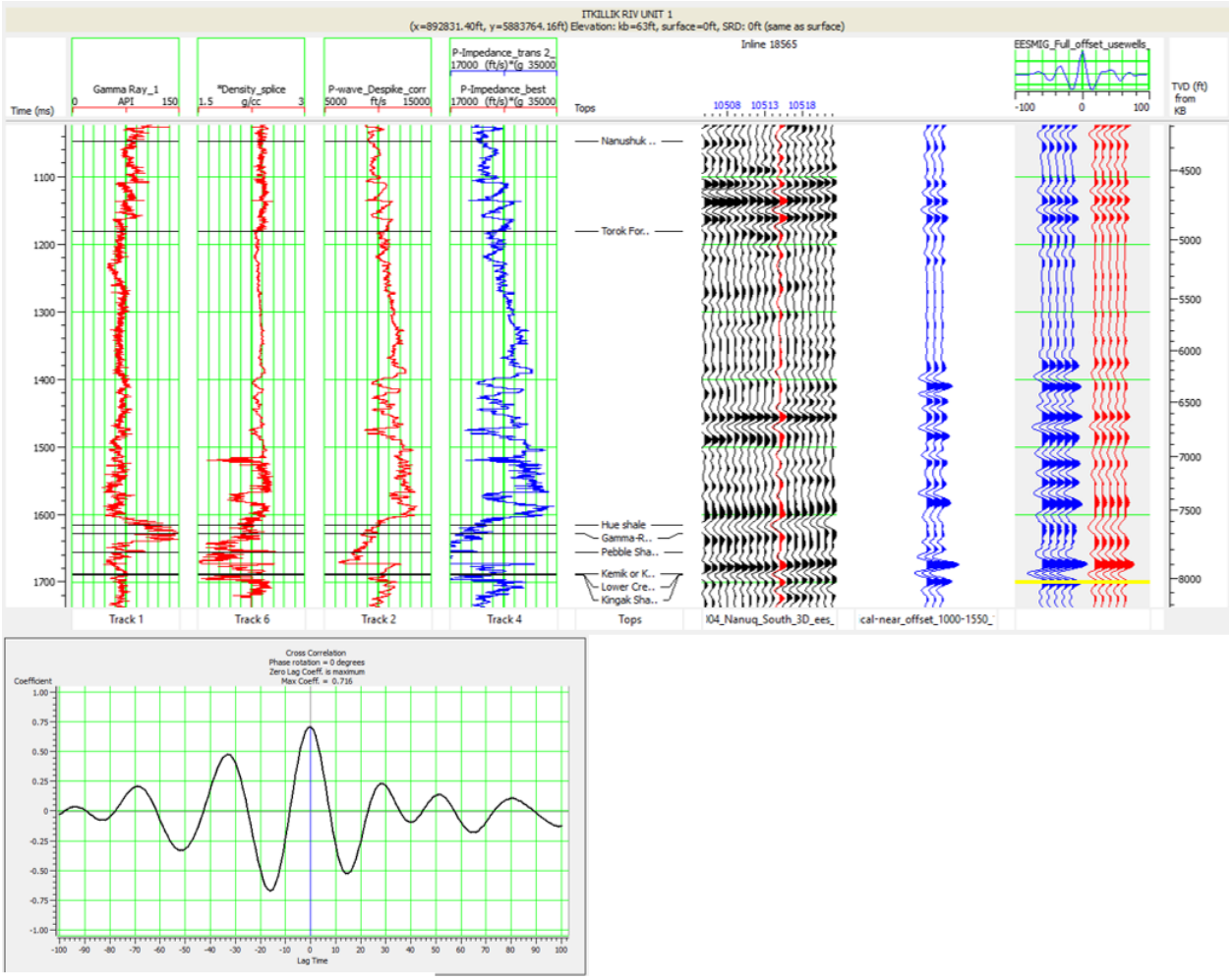

0.716 max correlation coefficient

Figure 5.17 Itkillik River Unit 1 seismic well tie. The far-right track shows the synthetic trace in blue alongside the extracted seismic trace in red. Ideally, the peaks and troughs would match in both position and amplitude. A correlation coefficient of 0.716 was achieved. This correlation coefficient describes the degree to which the blue synthetic trace and the extracted red trace match along depth.

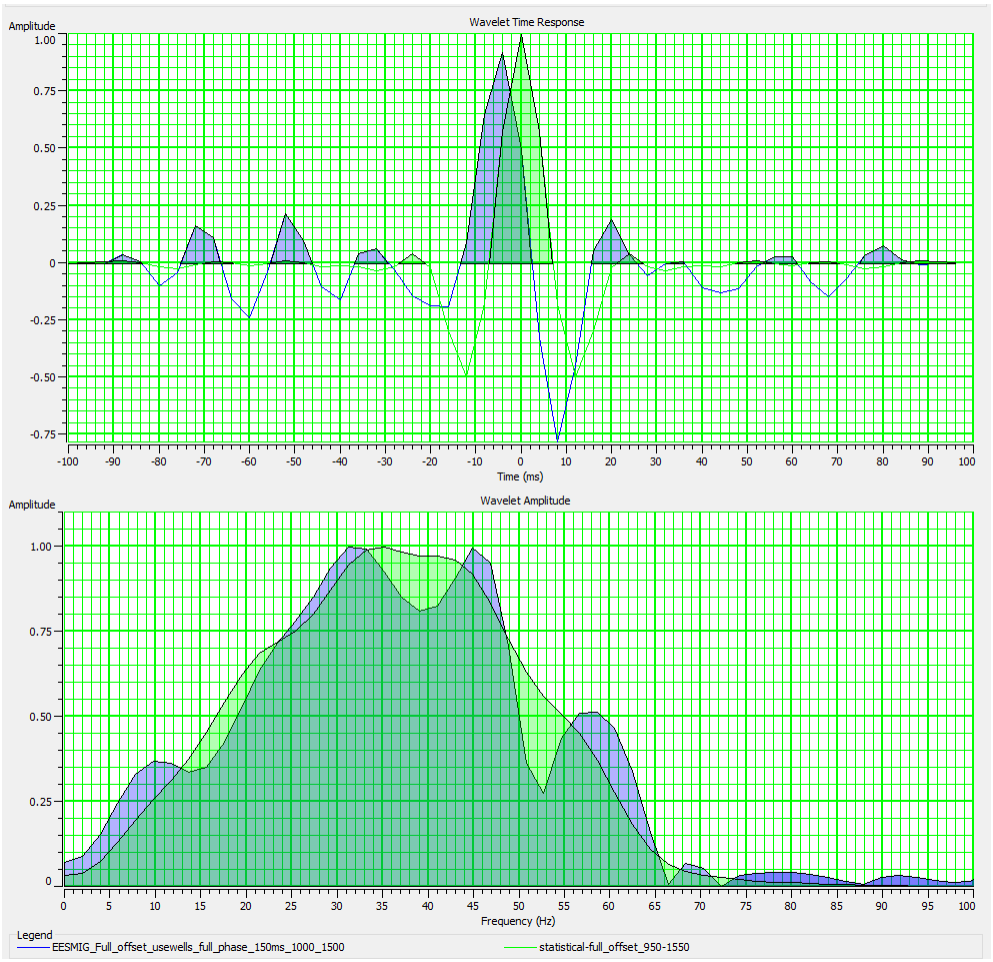

Figure 5.18 Final wavelet extraction - Nanuq South 3D seismic survey. The initial statistical wavelet extracted over the limited time window is shown in green, and the full phase wavelet extracted using wells is shown in blue. The blue wavelet provided a much better forward modeling result since it more accurately captures the frequency spectrum and acoustic behavior of the original trace data. Once the wells were initially correlated, a new wavelet was extracted at the well locations. This new wavelet was applied in the second phase of log correlation, and provided optimal results. The correlation between the synthetic seismic trace and the extracted trace jumped up from 0.61 minimum correlation to 0.97 minimum correlation.

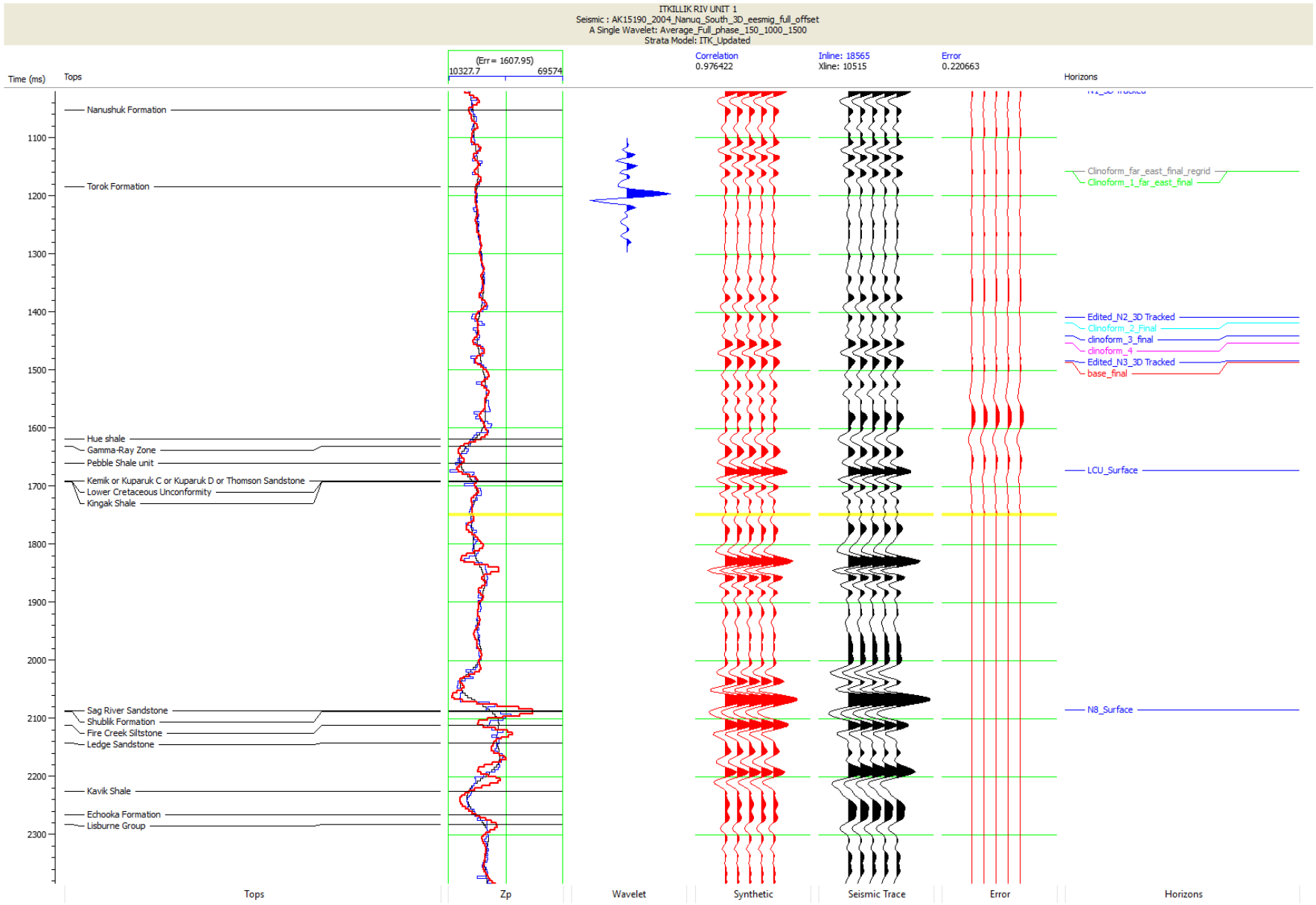
ITKILLIK RIV UNIT 1
Seismic : AK15190_2004_Nanuq_South_3D_eesmig_full_offset
A Single Wavelet: Average_Full_phase_150_1000_1500
Strata Model: ITK_Updated
Time (ms)
Tops
(Err= 1607.95)
10327.7
69574
Correlation
0.976422
Inline: 18565
Xline: 10515
Error
0.220663
Horizons
Nanushuk Formation
Torok Formation
Hue shale
Gamma-Ray Zone
Pebble Shale unit
Kemik or Kuparuk C or Kuparuk D or Thomson Sandstone
Lower Cretaceous Unconformity
Kingak Shale
Sag River Sandstone
Shublik Formation
Fire Creek Siltstone
Ledge Sandstone
Kavik Shale
Echooka Formation
Lisburne Group
Clinoform_far_east_final_regrid
Clinoform_1_far_east_final
Edited_N2_3D Tracked
Clinoform_2_Final
clinoform_3_final
clinoform_4
Edited_N3_3D Tracked
base_final
LCU_Surface
N8_Surface
1100
1200
1300
1400
1500
1600
1700
1800
1900
2000
2100
2200
2300
Tops
Zp
Wavelet
Synthetic
Seismic Trace
Error
Horizons

04

Figure 5.19 Final log correlation results - Itkillik River Unit 1 well. The far left track (track 1) shows the well log tops identified in the Itkillik River Unit 1 well. Track 2 contains the blue log-calculated impedance curve, the red inverted impedance result at the well location, and the black background model impedance curve. Track 3 contains the full phase wavelet used in the forward modeling and inversion modeling analysis. Track 4 contains the synthetic seismic trace generated by convolving the log-generated reflectivity series with the extracted full form wavelet. Track 5 contains the extracted seismic trace along the well path. Track 6 contains the residual data computed by determining the arithmetic difference between the synthetic trace and the extracted trace. Track 7 contains the time – depth value of the seismic horizons as they intersect the well path.

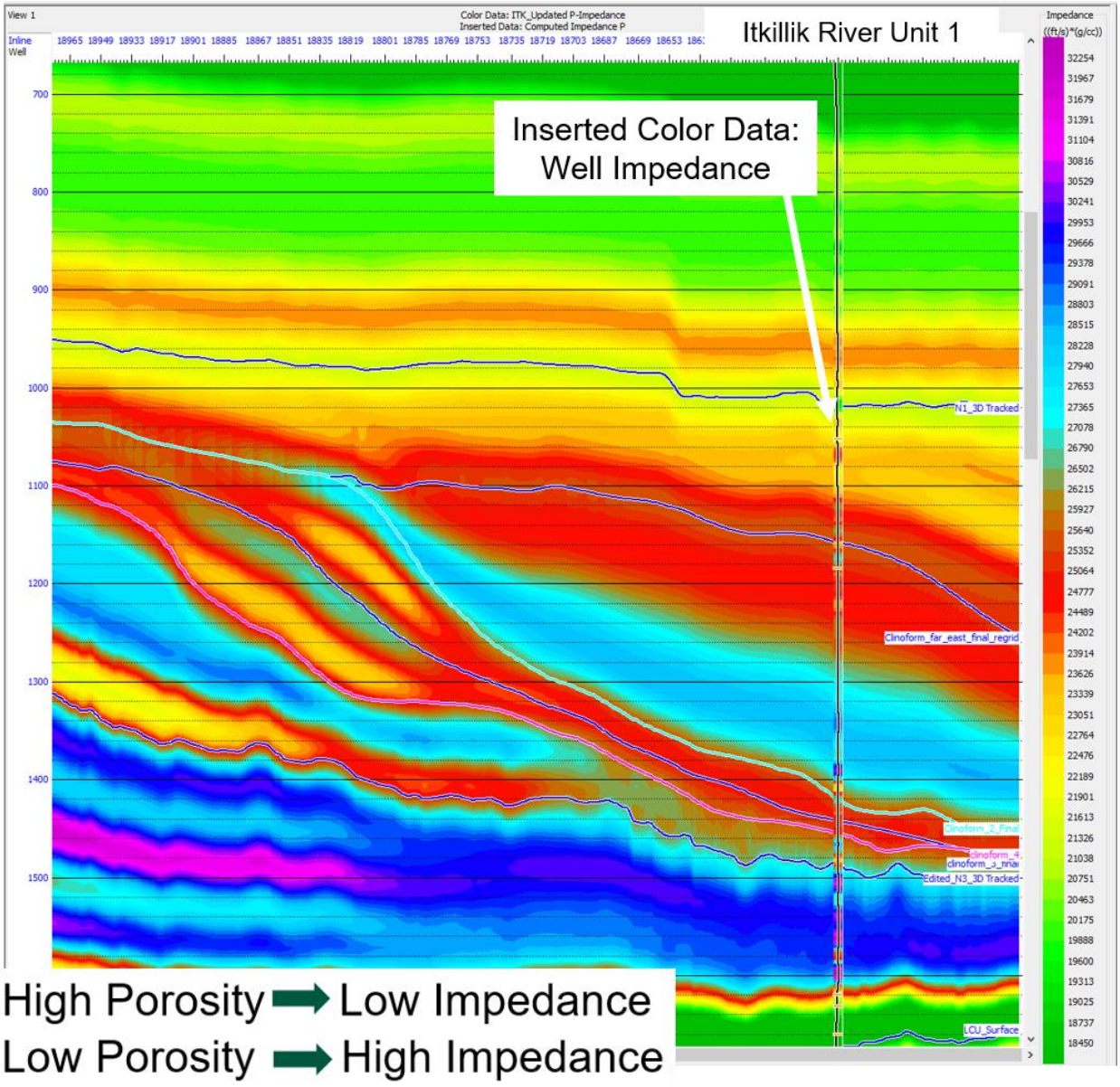

Figure 5.20 Impedance model generated using only the Itkillik River Unit 1 well. This impedance cross section shows the well impedance data inserted into the section. For this project, only the Itkillik River Unit 1 well was used to train the background model. To visually inspect the fit of the model, compare the impedance response calculated at the well section to the modeled data (pink is high impedance, low porosity and green is low

impedance, high porosity) Since this model was trained using the Itkillik River Unit 1 well, it is expected that this model is a good fit to the log calculated data across the time window of interest (750ms – 1750ms) corresponding to the Brookian Section. The seismic horizons are used as a guide to allow the model to interpolate impedance values between well locations. The model initiates at the input well location, and then uses the horizons as a guide, painting impedance values based on the nearest well result and stretching or squeezing the data as necessary to fit within the bounds of the seismic horizons. The clinothem bounded by clinoform surfaces at approximately 1100 and 1400 ms exhibits a zone of lower impedance (red zone) above a zone of higher impedance (turquoise zone). The geometry of these differing impedance zone mimics the geometry of the relative distribution of systems tracts within the bounded clinoformal surfaces.

5.3.2 The Inverse Model

Simply stated, the goal of seismic inversion is to relate each individual seismic trace to the actual rock properties represented at the trace location (primarily V_p, V_s, density, AI, and porosity). Once the forward seismic modeling results correlated with the original seismic trace data, the relationship between acoustic impedance and the seismic trace was propagated through the whole seismic volume to generate the intial model (Figure 5.20). Numerous models were generated, with each iteration using a different well or wells to train each initial model.

Ultimately, a model using only the Itkillik River was chosen for the final inversion. Pre-inversion analysis indicated that the inversion process should return usable results, based on the correlation analysis performed by plotting the inverted impedance versus the original impedance at each well location for all wells in the study area (Figure 5.21). The correlation between the synethic seismic trace and the original seismic trace was greatly improved across the study area, with the minimum correlation coefficient increasing fro 0.61 to 0.97, resulting from switching from the statistical wavelet to the full phase wavelet extracted using wells. This increase in correlation is likely due to the fact that wavelet used in the second phase of log correlation was based on the data at individual well location after the initial correlation was made as opposed to a statistical wavelet that can be used to “describe” the whole seismic area.

The seismic trace data was then inverted using the final extracted full phase wavelet from the forward modeling process (Figure 5.18). This seismic inversion process, guided by the interpreted horizons and the initial model, generated an impedance volume, with an inverted acoustic impedance response at each trace.

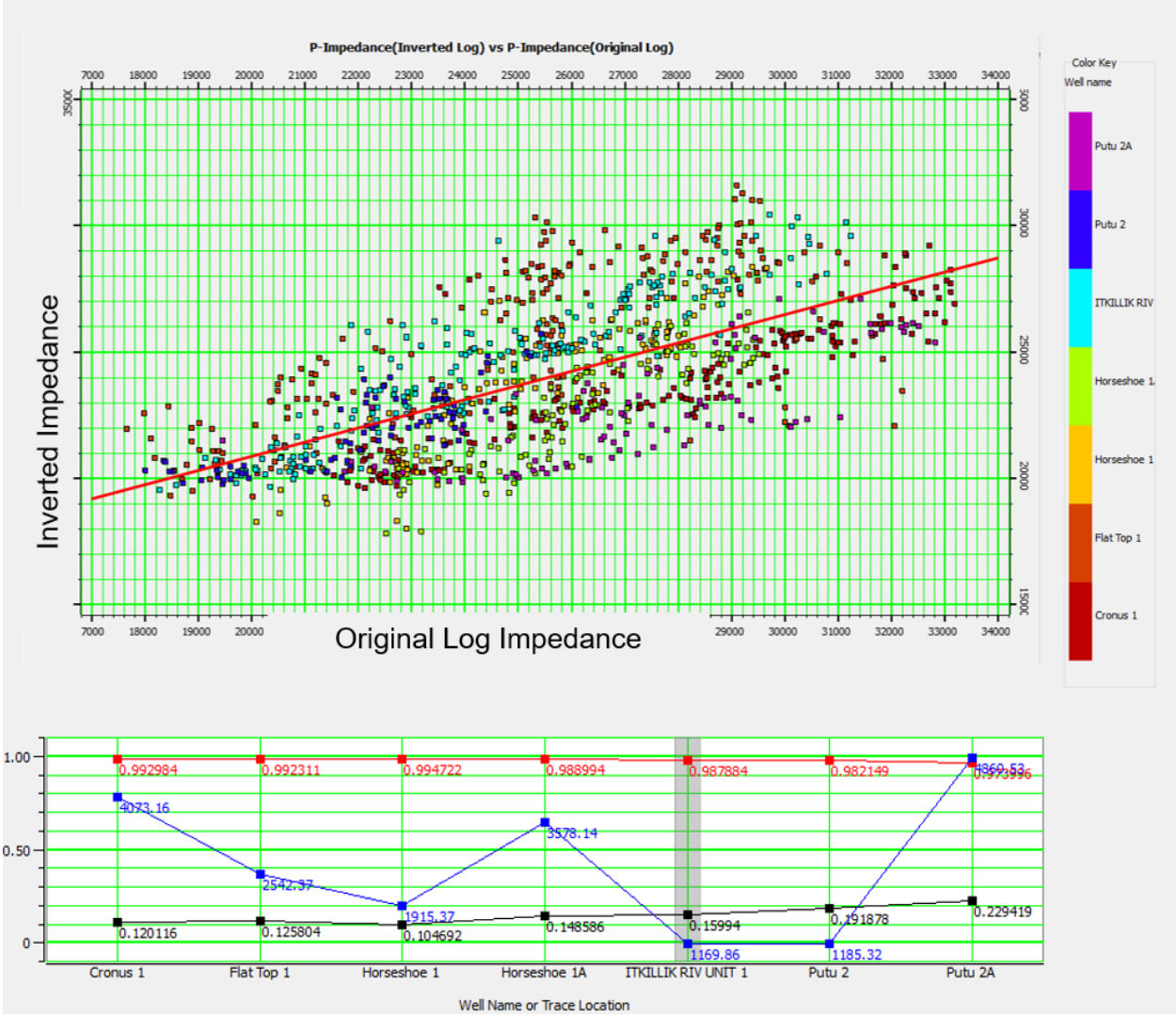

Figure 5.21 Inverted log impedance vs. original log-calculated impedance, all well locations. The cross-plot at the top of this figure plots the original log-calculated impedance on the x-axis, the inverted impedance on the y-axis, and the data is colored by well location. There is a degree of correlation between these two values, and a trend line representing the data is shown is red. The lower error plot graph visualizes the errors present at each well location. The red line indicates the degree to which the synthetic seismic matches the extracted trace at the well location. This graph indicates

a great correlation was achieved across the study area, with a minimum correlation of .97. The blue line indicates the amount of error between the inverted impedance values and the well calculated impedance values. Lower values for this error are ideal, and the lowest error is predictably present in the Itkillik River 1 well. This error could be improved by blocking the density and velocity logs prior to generating an impedance curve to mimic the blocky nature of the seismic data, caused by a coarser resolution. The black line illustrates the amount of error between the inverted impedance volume and the original trace data. Ideally, this error should be as close to zero as possible.

Visual inspection of the inversion results at the Itkillik River Unit 1 well location indicates that valid results were achieved at this well location, but this is expected given this well was used to train the background model (Figure 5.22). These results could be improved by refining the seismic to well correlation along the entire path of borehole, since for the purposes of this study, the focus of correlation was just on the Brookian Section (approximately 750 ms – 1750 ms).

Ideally, the inverted impedance volume would closely match the inserted log-measured impedance for all wells, including the “blind” wells not used to train the model. In order to validate the results, well-based acoustic impedance was visualized alongside the inverted impedance data at the Putu 2, Putu 2A, Horseshoe 1, and Horseshoe 1A well locations.

Impedance results at the Horseshoe 1 well location partially provide a reasonable validation for a limited range of depths of the inverted volume. The visual inspection of this data indicates a reasonable match between the calculated log inversion data and the inverted impedance volume from approximately 750ms to 1110ms along the Horseshoe 1 well path (Figure 5.23). The main reservoir intervals at the Horseshoe 1 well are the Nanushuk 5 and the Nanushuk 3 zones. Based on the lack of low impedance anomalies detected in the log-calculated impedance data, these reservoir zones do not have a strong enough acoustic response to produce a clearly delineated boundary between the reservoir and the surrounding rock volume. Despite this lack of strong acoustic response, the inverted impedance volume does match the inserted well data at the penetrated reservoir depths.

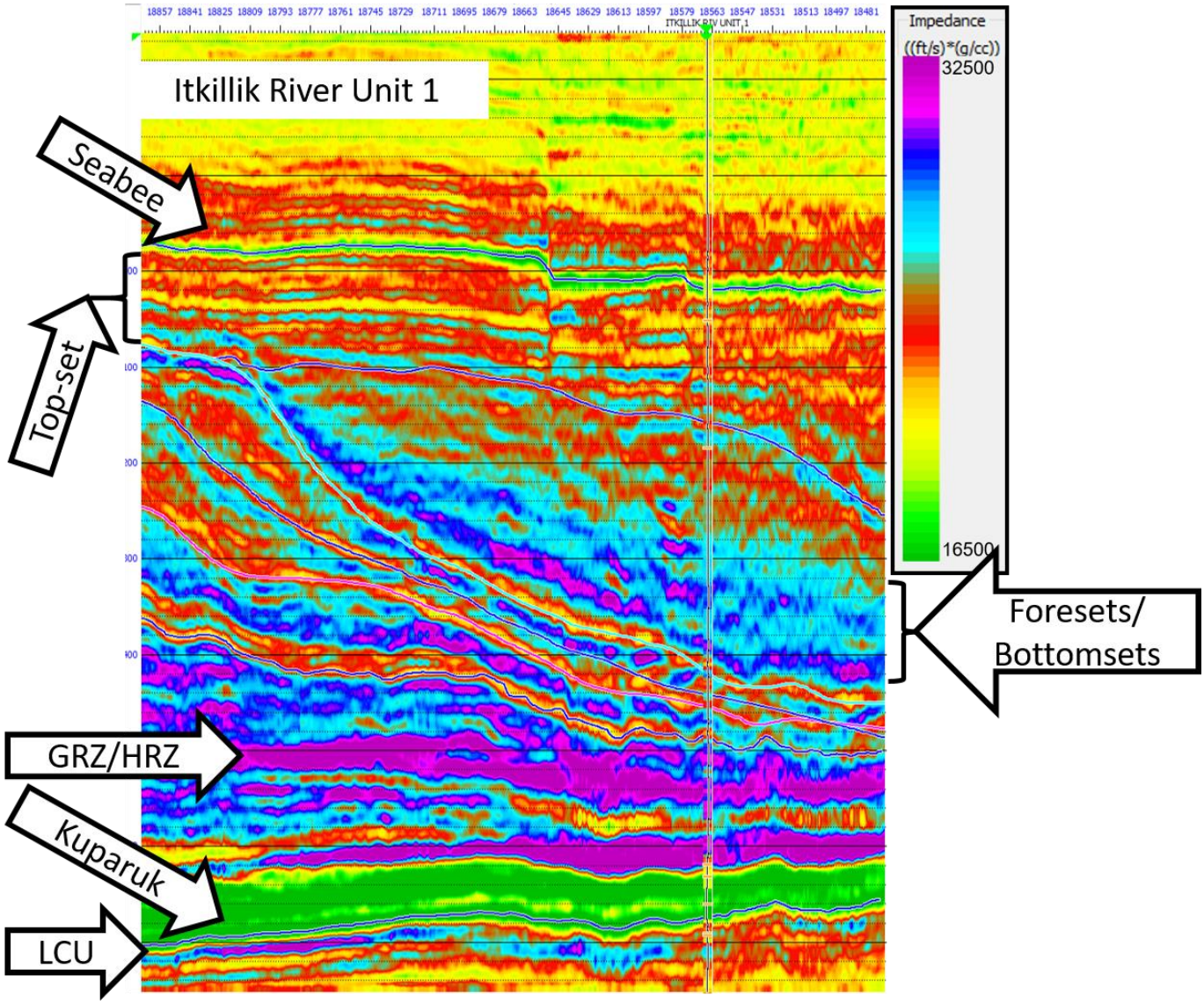

Figure 5.22 Inverted impedance section at the Itkillik River Unit 1 well location. Low impedance (visualized with yellows and greens) values are indicative of higher porosity or lower clay/silt content zones. High impedance (visualized with pinks and dark blues) are indicative of lower porosity or higher clay/silt content. Visual inspection of the inserted log impedance along the well path in comparison to the inverted impedance result indicates a good match between the two datasets. This is expected because the

Itkillik River Unit 1 well the only well used to train the model used to guide the inversion process through the data volume. The main reservoir interval penetrated by this well is the Kuparuk section, visualized near the base of this inversion display as a low impedance layer (green). This low impedance section is detected throughout the inverted volume.

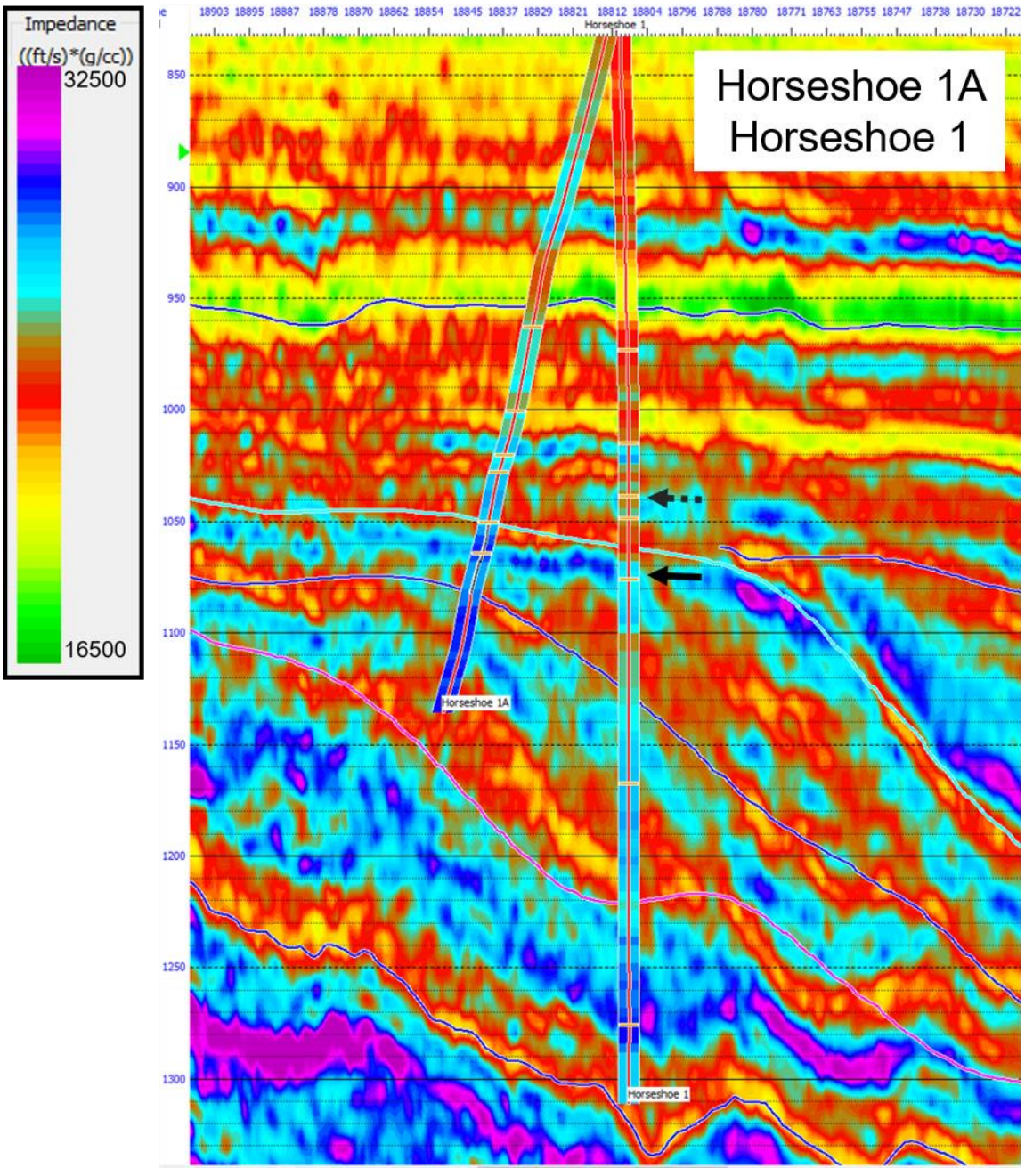

Figure 5.23 Inverted impedance section at the Horseshoe 1 and Horseshoe 1A well locations. Low impedance values (visualized with yellows and greens) are indicative of higher porosity or lower clay/silt content zones. High impedance values (visualized with pinks and dark blues) are indicative of lower porosity or higher clay/silt content.

Horseshoe 1A is plotted on the left side of this display and is a deviated borehole. There is no correlation between the log-calculated impedance and the inverted impedance volume, as is evidenced by visually inspecting the colored impedance response along the Horseshoe 1A well. Horseshoe 1 is plotted to the right of Horseshoe 1 and is an effectively straight borehole. The solid black arrow indicates the position of the main reservoir interval for the Horseshoe 1 well, the Nanushuk 3 zone. The dashed black arrow indicates the position of the secondary reservoir interval in the Horseshoe 1 well, the Nanushuk 5 zone. The visual correlation between the inverted impedance response and the well impedance indicates a partial correlation, with the events at ~950 ms, 1015 ms, and 1050 ms exhibiting a similar acoustic impedance response in both the inverted and log-calculated impedance datasets. Note: as a predictive tool, the inverted volume would have not indicated the presence of the reservoir penetrated by the Horseshoe 1 well, however, the well results also do not indicate anomalously low impedance in the reservoir zone.

The visual inspection of the impedance results at the Horseshoe 1A well location does not validate the inverted impedance result (Figure 5.23). The low impedance zone between two layers of higher impedance is detected at approximately 950 ms at the Horseshoe 1A well location, but the absolute value of the impedance as determined by the inserted log-calculated impedance value is almost an order of magnitude higher than the absolute impedance indicated by the inverted volume. The results at this welll location could be improved by limiting error introduced by the researcher, and ensuring the well-tie process is performed correctly on this deviated well and using the regenerated P-wave velocity from the corrected well tie to recompute the well-based acoustic impedance. This recomputed well-based acoustic impedance could then be re-inserted at this well location, potentially providing a better visual match and validating the results at this well location.

The visual inspection of the inverted impedance section and the inserted log impedance values at the Putu 2 and Putu 2A well location does not validate the inverted impedance result (Figure 5.24). While the inverted acoustic impedance at the Putu 2 location does provide a marginally better visual match to the inserted log-calculated impedance, that match is pattern based at best and still could not reasonably be described as validating the inversion result based on the blind well test. Inspection of the log-calculated acoustic impedance reveals a signficiant problem with the log calculated impedance at the Putu 2 and 2A well locations: there is no obvious indication on either log measured impedance of the “Narwhal Sand”, a productive hydrocarbon zone penetrated by both wells. Despite the well logs not detecting the productive zone, the inverted impedance volume does indicate an anomalously low zone of acoustic

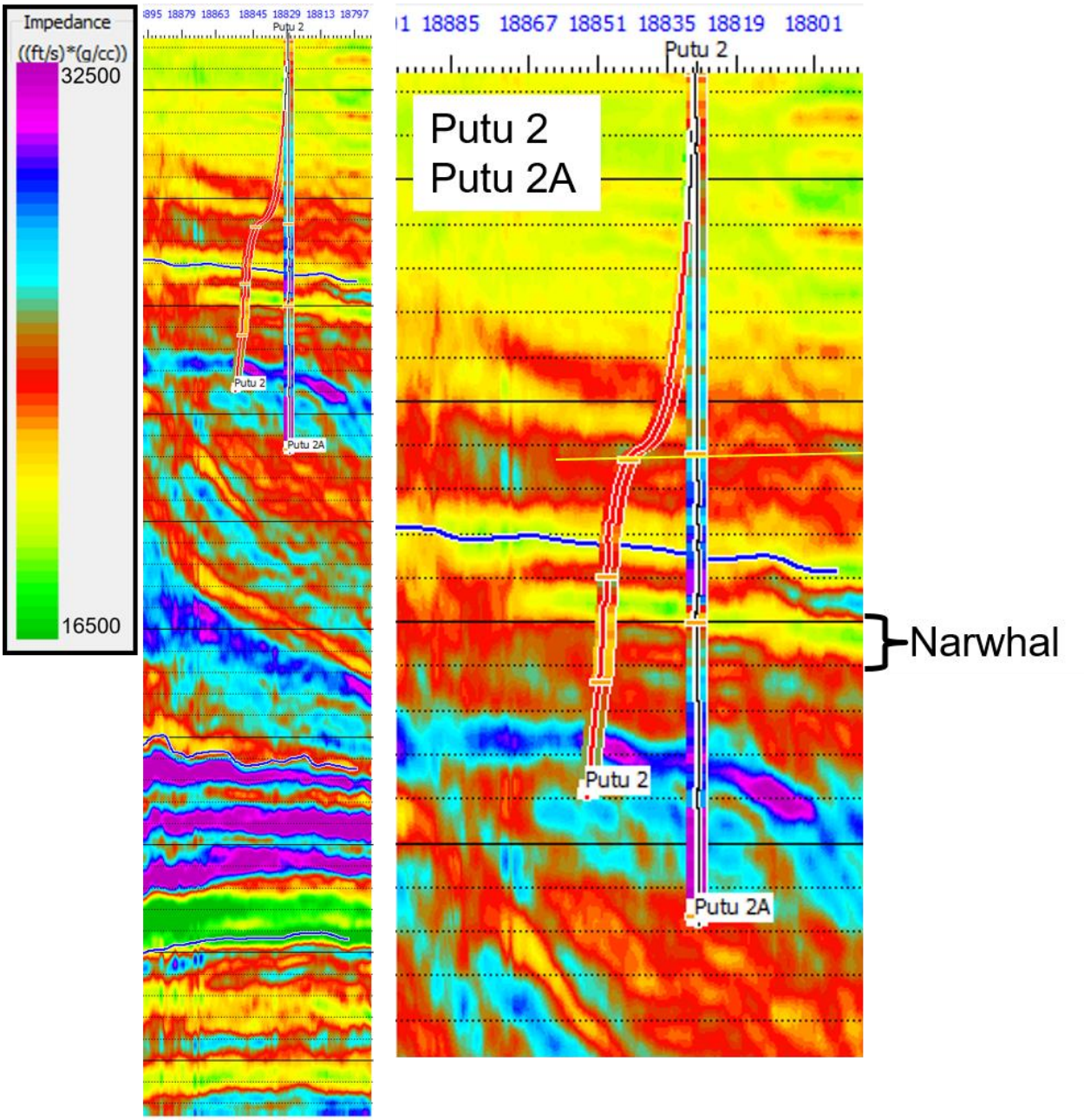

Figure 5.24 Inverted impedance section at the Putu 2 and Putu 2A well locations. Low impedance values (visualized with yellows and greens) are indicative of higher porosity or lower clay/silt content zones. High impedance values (visualized with pinks and dark blues) are indicative of lower porosity or higher clay/silt content. While the Putu 2

inserted log impedance provides a better match as compared to the Putu 2A inserted well impedance, neither well acts to validate the inversion result. However, there is an anomalously low zone of acoustic impedance detected by the inverted impedance volume that directly corresponds to the Narwhal Sand as penetrated by the Putu 2 and Putu 2A boreholes. The Narwhal sand is a Nanushuk equivalent formation. Despite the blind well test failing for both Putu 2 and Putu 2A likely due to data issues, the results of the well act to validate the inverted volume, since the inverted impedance volume detects a local low impedance event corresponding to the productive reservoir interval as penetrated by these two wells.

impedance displayed in green directly below the blue horizon. This low acoustic impedance zone likely corresponds to the productive Narwhal Sand, a Nanushuk equivalent oil-bearing reservoir.

The remaining two study area wells (Cronus 1 and Flat Top 1) were not within the boundaries of the Nanuq South 3D seismic survey, so these two wells were not inspected as blind well for validation of the inversion results.

The final step in this project involved generating a porosity volume based on the relationship between log-calculated average porosity and log-calculated acoustic impedance at the Itkillik River Unit 1 well location (Figure 5.25). Because there was no core taken from Itkillik River Unit 1's Brookian section, there was no option to calibrate the log-calculated porosity to core-measured porosity values, and the resultant porosity volume contains erroneously high porosity values, some of which are theoretically impossible to achieve at the depths included in the porosity volume. In its current state, this porosity property cube cannot be used as a quantitative tool for reservoir characterization, since the absolute porosity values indicated in the volume are not theoretically possible at depth for consolidated rocks. However, this porosity data volume does have value as a qualitative assessment tool, and can be used as a relative porosity indicator.

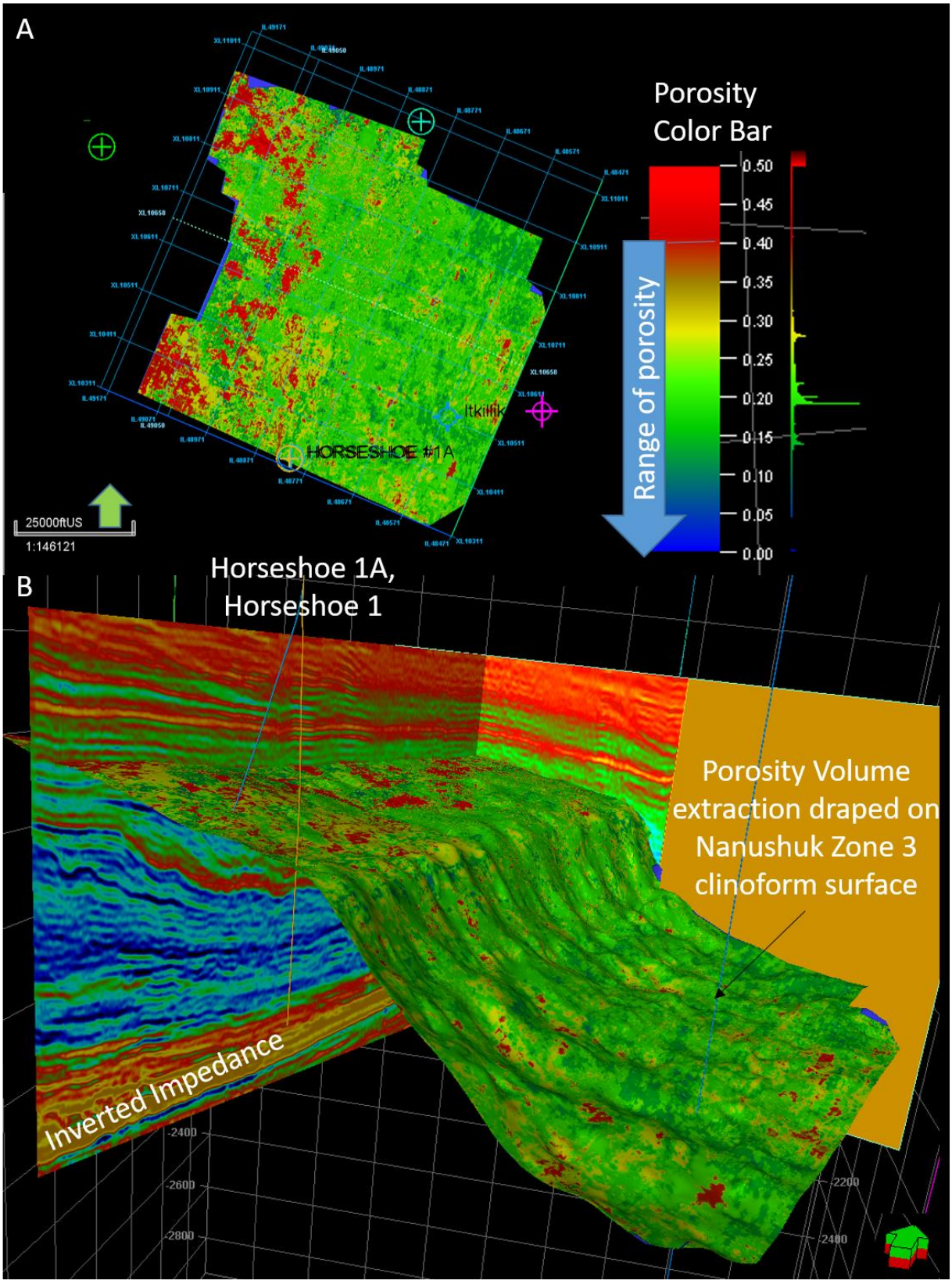
A
Porosity
Color Bar
0.50
0.45
0.40
0.35
0.30
0.25
0.20
0.15
0.10
0.05
0.00
Range of porosity
Itkillik
HORSESHOE #1A
25000ftUS
1:146121
B
Horseshoe 1A,
Horseshoe 1
Porosity Volume
extraction draped on
Nanushuk Zone 3
clinoform surface
Inverted Impedance
-2400
-2600
-2800
-2200
-2400

Figure 5.25 Porosity property volume visualization.

A. The upper portion of this figure illustrates the porosity property draped on a three dimensional visualization of the Nanushuk Zone 3 surface, the main reservoir interval of the Horseshoe 1 well. The color bar applied is displayed on the right side of the upper panel, and demonstrates the range of values indicated in the property volume, with reds corresponding to high porosity, and greens corresponding to low porosity. Since the maximum theoretical porosity achieved in experiments using perfectly sorted spheres is 47.6% in cubic arrangement and 39.5% in a hexagonal arrangement, all values greater than 39.5% are theoretically impossible exclusive of instances of vuggy porosity, which is not anticipated to exist in this study area. The porosity volume has value only as a qualitative tool, as it is possible to delineate areas of higher porosity as compared to the background response, however absolute porosity values extracted from this data volume should not be used quantitatively.

B. The extracted value of the porosity volume has been gridded and draped over the Nanushuk 3 clinoform surface. An inline and crossline from the inverted impedance volume are displayed as a backdrop to the porosity data. Qualitatively, areas colored red correspond to higher porosity values, and areas colored green correspond to lower porosity values.

6. Discussion

The results from the initial seismic interpretation and seismic attribute extraction indicated that the amplitudes preserved in the Nanuq South 3D seismic survey were geologically relevant. Geologically relevant amplitudes follow imaged structures, and occur in predicable locations based on the geologic knowledge of the area. In the case of this study, strong RMS amplitude anomalies are anticipated to occur primarily within the topset facies of the Nanushuk formation, with some additional high amplitude anomalies within the foreset and bottomset facies of the Torok Formation. The results of the seismic attribute extraction indicated that these high RMS amplitude anomalies exist in spatially relevant areas, and provide the first measure of assureness that a seismic inversion workflow applied to the Nanuq South 3D dataset could yield meaningful results.

While extracting seismic attributes generates a quick, on the fly, visual display capable of highlighting areas of strong RMS amplitude response, a more robust analysis is required to reveal quantifiable internal layer properties. The seismic attribute display has the potential to indicate the presence and location of the boundary between hydrocarbon accumulations and non-hydrocarbon bearing formations, however, these attribute displays do not tell the whole story. Reflectivity from conventional seismic data relays information about the interface between two layers with contrasting impedance, but does not give us information about the internal layer properties. In order to extract additional information aside from the approximate “depth” to a potential hydrocarbon target, a robust and integrated petrophysical analysis and subsequent seismic inversion

workflow is required to analyze interal layer properties, specifically porosity and/or lithology (relative clay content).

The results of the basic petrophysical study highlighed the utility of “on the fly” cross-plot generation. Cross-plots allow the interpreter to instantly visualize the relationship between two often large data sets in order to highlight trends in the data. Cross-plots also act as a quality control tool to highlight problems within the data. After generating the computed log properties discussed in this volume and cross-plotting properties of interest, the petrophysical data was used as an input for statistical mineralogical modeling. The results of the petrophysical modeling highlighted the need to ensure that critical calcuations, especially water saturation, is performed intelligently, using the geologic background knowledge of the study area. For this project, using Simandoux’s equation for water saturation in low resistivity, shaly sandstone reservoirs provided a much better fit to the core-measured water saturation data. Additionally, this study demonstrated that the application of a robust statistical modeling workflow was capable of mimicing the results of expensive spectroscopy log responses. The Horseshoe 1 well contained spectroscopy log information that was used to validate the result of statistical mineralogical modeling using standard geophysical log curves. The visual inspection of the modeled volumetic mineral and pore fluid content indicated a reasonable correlation with the log-measured volumetric mineral and pore fluid content, exclusive of detecting the volumetric distribution of limestone. This mineralogy was not included in the model as a possible lithology. Based on the fact that the statistical mineralogical modeling results from the Horseshoe 1 well correlated with the results from the spectroscopy logs, the statistical modeling results from the other well locations

can be used with confidence, since similar parameters were used for each of the study wells.

Once both the initial seismic interpretation and the robust petrophysical analysis was completed, the data generated from those activities was exported from Petrel™ and PowerLog™ into Hampson Russell™ for use in the post-stack seismic inversion workflow. When visually inspecting amplitudes extracted from the post-stack Nanuq South 3D conventional reflection seismic volume, instances of strong amplitude response provide the interpreter with information about the spatial location and “depth” at which a potentially hydrocarbon bearing interval begins based on the visualized reflectivity contrast. In the case of inverted data, strong impedance responses are associated with the internal rock properties of the formation, making inverted data ideal for stratigraphic interpretation, since the inverted impedance data tells us not only the depth and location of impedance anomolies, but also provides continuous absolute impedance values at every depth along every trace across the entire seismic volume. This continuous record of absolute impedance values allows the interpreter to quantitatively describe interal layer properties.

The model-based inversion workflow performed for this study was based on a model generated soley using data from the Itkillik River Unit 1 well, a wavelet, and six regional clinoformal surfaces. The Itkillik River Unit 1 well, which was drilled in 1978, contains data of a quality that is prevalent across the entire state of Alaska. While it is highly likely that a better inversion result could have been achieved by basing the background model used to train the inversion process on one of the more modern wells with better data, the choice to use a legacy well was purposeful so results of this study

could be used as “proof of concept” that modern well data is not required to produce meaningful seismic inversion results. While the inverted impedance results were only validated with one of five blind well tests, the inverted impedance volume did effectively detect the Narwhal Sand, the productive hydrocarbon-bearing reservoir interval penetrated by the Putu 2 and Putu 2A wells.

The porosity property cube generated in this study contains erroneously high porosity values, some of which are not statistically possible. As such, it would not be advisable to utilize the porosity volume as a quantitative tool for describing porosity. However, the porosity volume does have value as a qualitative tool, highlighting areas within the volume that have higher porosity relative to the background lower porosity response.

Improvements to the project could generate better results from the seismic inversion workflow. There were some data quality issues that arose within the Putu 2 and Putu 2A well datasets which potentially impacted the quality and accuracy of the log-calculated impedance response from this borehole. Additionally, more work could be done to improve the relationship between porosity and acoustic impedance as derived from the Itkillik River Unit 1 well data. This improvement could then be used to regenerate the porosity volume, potentially yielding results suitable for quantitative interpretation, assuming the correction produces values that fall within the realm of theoretically possible porosity values.

Despite the flaws present in both the inverted impedance volume and the transformed porosity volume, both data volumes are valuable data sources to inform regional resource volume assessment activities. Assessors can visualize and

manipulate the inverted impedance data in order to better evaluate the chance of geologic success of Brookian reservoirs on Alaska's North Slope. Additionally, this workflow could be repeated anywhere in the region, as long as at least one well is present within the boundary of a modern 3D seismic survey with geologically relevant preserved amplitudes.

Despite being trained on well data from a well drilled in 1978, the inverted impedance volume resulting from the model-based inversion of the Nanuq South 3D survey successfully detected the primary reservoir interval targeted by the Putu 2 and Putu 2A wells, both drilled nearly four decades after the Itkillik River Unit 1 training well was completed. Further work could be performed to determine why this proven Brookian reservoir interval from the Putu wells was delineated, while the proven Brookian reservoir interval from the Horseshoe well locations was not delineated.

7. Conclusions

The results of this study demonstrate that the inverted impedance volume resulting from post-stack model-based seismic inversion workflow can detect hydrocarbon bearing intervals, as evidenced by the detection of the Narwhal sand, the productive interval penetrated by the Putu 2 and Putu 2A boreholes. This model-based inversion was guided using a background model based on data from the Itkillik River Unit 1 well, a legacy well drilled in 1978. The vintage log-suite contains data of a quality that is prevalent acrosss the state of Alaska. Because the inverted impedance volume infused with legacy well data was able to detect at least one known hydrocarbon accumulation, this study serves as proof of concept that legacy well data can be used to train a background model and ultimately produce a meaningful inversion result. Of course, if modern well data is available, utilizing well data collected by technologically advaced tools would likely provide a better result, but modern well data is not readily avaibale across Alaska's plentiful propsective basins.

Additionally, the results of this study indicate that the use of statistical mineralogical modeling could have far-reaching impacts for North Slope exploration, since many wells in the region have limited log data and a high incidence of missing curves. By applying a similar statistical mineralogical modeling workflow to other legacy well datasets, additional information can be extracted from vintage datasets, mimicing the results of expensive spectroscopy logs..

8. Recommendations for Future Work

The seismic survey used in this study is one of many 3D seismic volumes available through the State of Alaska's Tax Credit Seismic Program imaging portions of the Colville foreland basin. Three additional 3D seismic volumes in the area have a number of on-seismic wells with publicly available well data to expand this study across the Colville foreland basin: NE NPR-A 3D, Smith Bay 3D, and Umiat 3D.

Pre-stack seismic data (angle gathers) are available for public use through the State of Alaska's Tax Credit Seismic Program for all four seismic surveys referenced in this section. A future project utilizing the results of pre-stack seismic inversion could yield additional, unique property volumes (Poisson's ratio, bulk modulus, and Young's modulus cubes) that would aid in further reservoir characterization.

A robust, integrated petrophysical and seismic inversion study utilizing regional well and seismic data has the potential to reveal trends in reservoir quality as related to sediment provenance in the region. Multiple USGS studies involving detrital zircon analysis of core samples, thin section analysis, and regional qualitative seismic analysis supports the hypothesis of dual concurrent sources of sediment influx to the Colville foreland basin (Houseknecht et al., 2019). A future inversion study could be used to build on the dual sediment source hypothesis and determine if there is a quantifiable difference between the seismic amplitudes related to the coarse-grained, hydrocarbon bearing sediments deposited from uplift related to the Chukotka orogeny in the western portion of the study area as compared to the amplitudes related to those with a relatively higher influx of sediments deposited from uplift related to the Brooks Range orogeny in the south and south-eastern portion of the study area.

9. References Cited

Alaska Department of Natural Resources Division of Oil and Gas, 2021, GIS Data, https://dog-soa-dnr.opendata.arcgis.com/ (accessed February 1, 2021).

Alaska Geologic Materials Center, 2019, Seismic and Well Data: https://dggs.alaska.gov/gmc/seismic-well-data.php (accessed September 15, 2019).

Bailey, B., Barclay, F., Nesbit, R., Paxton, A., 2010, Prospect Identification using AVO Inversion and Lithology Prediction (abs): ASEG Extended Abstracts, v. 2010, no. 1, p. 1-4.

Barclay, F., et al., 2008, Seismic Inversion: Reading Between the Lines: Schlumberger Oil Field Review, https://www.slb.com/-/media/files/oilfield-review/seismic-inversion (accessed April 15, 2021).

Bhattacharya, S., and Verma, S., 2020, Seismic attribute and petrophysics-assisted interpretation of the Nanushuk and Torok Formations on the North Slope, Alaska: Interpretation, v. 8, no. 2, p. 17-34.

Bird, K., 2001, Framework geology, petroleum systems, and play concepts of the National Petroleum Reserve - Alaska, *in* D. W. Houseknecht, ed., Petroleum Plays and Systems in the National Petroleum Reserve – Alaska: SEPM Special Publication 21, p. 5-17.

Caf, A. B., and Pigott, J. D., 2016, Seismic Stratigraphic and Quantitative Interpretation of Leonardian Reefal Carbonates, Eastern Shelf of the Midland Basin: Insight Into Sea Level Effects, Geomorphology and Associated Reservoir Quality: Search and Discovery Article #10909, http://www.searchanddiscovery.com/pdfz/documents/2017/10909caf/ndx_caf.pdf.html (accessed October 19, 2019).

Chaouch, A., and Mari, J.L., 2006, 3-D Land Seismic Surveys: Definition of Geophysical Parameters: Oil and Gas Science and Technology, v. 62, no. 5, p. 611-630.

Chaveste, A., and Hilterman, F., 2007, Well-log inversion and modeling - A tool for understanding ambiguity and sensitivity of seismic data to changes in petrophysical properties: The Leading Edge, v. 26, no. 7, p. 812-817.

Chopra, S., and Marfurt, K., 2007, Seismic Attributes for Prospect Identification and Reservoir Characterization: Tulsa, Society of Exploration Geophysicists, 464 p.

Decker, P. L., 2018, Nanushuk Formation Discoveries: World class exploration potential in a newly proven stratigraphic play, Alaska North Slope: https://dog.dnr.alaska.gov/Documents/ResourceEvaluation/20180521_DiscovThinking_Decker.pdf (accessed October 10, 2019).

ESRI, 2021, World Imagery Map Service: https://www.arcgis.com/home/item.html?id=10df2279f9684e4a9f6a7f08febac2a9 (Accessed February 15, 2021).

Gregersen, L. S., and Brown, G. A., 2019, Map and Database of Exploration Drilling Targets Categorized by Play Type, North Slope and Offshore Arctic Alaska: Alaska Department of Natural Resources, Division of Oil and Gas: https://dog.dnr.alaska.gov/Information/Studies (accessed June 4, 2020).

Helmold, K. P., 2016, Sedimentary petrology and reservoir quality of Albian-Cenomanian Nanushuk Formation sandstones, USGS Wainwright #1 test well, western North Slope, Alaska, *in* LePain, D. L., ed., Stratigraphic and reservoir quality studies of continuous core from the Wainwright #1 coalbed methane test well, Wainwright, Alaska: Alaska Division of Geological & Geophysical Surveys Report of Investigation, p. 37-57.

Homza, T.X., 2004, A structural interpretation of the Fish Creek Slide (Lower Cretaceous), northern Alaska: AAPG Bulletin, v. 88, no. 3, p. 265-278.

Houseknecht, D. W., Bird, K. J., and Schenk, C. J., 2009, Seismic analysis of clinoform depositional sequences and shelf margin trajectories in Lower Cretaceous (Albian) strata, Alaska North Slope: Basin Research, v. 21 no. 5, p. 644-654.

Houseknecht, D. W., 2019, Petroleum systems framework of significant new oil discoveries in a giant Cretaceous (Aptian-Albian) clinothem in Arctic, Alaska: AAPG Bulletin, vol. 103, no. 3, p. 619-652.

Hudson, T., Nelson, P., Bird, K., and Huckabay, A., 2006, Exploration History (1964-2000) of the Colville High, North Slope, Alaska: Alaska Division of Geological and Geophysical Surveys Miscellaneous Publication 136, 32 p.

Magoon, L.N., The Petroleum System – Status of Research and Methods, 1992: Denver, US Geological Survey, 108 p.

Narbors, 2017, Horseshoe 1 Final Well Report, prepared for Armstrong Energy, LLC by Narbors Alaska Drilling, Inc., 72 p.

Ramon-Duenas, C., Rudolph, K.W., Emmet, P.A., and Wellner, J.S., 2018, Quantitative Analysis of siliciclastic clinoforms: An example from the North Slope, Alaska: Marine and Petroleum Geology, v. 93, p. 127-134.

Rose, P., 1992, Chance of Success and Its Use in Petroleum Exploration, in The Business of Petroleum Exploration: AAPG Treatise in Petroleum Geology, p. 71-86.

Russel, B.H., 2017, Stochastic vs Deterministic pre-stack inversion methods, CGG: https://www.cgg.com/data/1/rec_docs/3414_3412_Stochastic_vs_Deterministic_Inversion_Russell.pdf (accessed October 27, 2019).

Russel, B.H., and Hampson, D.P., 1991, A comparison of post-stack seismic inversion methods [abs.]: SEG Annual Meeting Abstracts, p. 876-878.

Sherwood, K.W., Craig, J.D., Cooke, L.W., et al., 1998, Undiscovered Oil and Gas Resources, Alaska Federal Offshore: Minerals Management Service, OCS Monograph MMS 98-0054, 511 p.

State of Alaska, Department of Natural Resources, Division of Oil and Gas, AS 43.55 Exploration Tax Credit Project 2017: http://dog.dnr.alaska.gov/Information/Geological/GeophysicalData (accessed September 15, 2019).

WesternGeco, 2004, Data Processing Report (Nanuq South 3D Seismic Survey), prepared for ConocoPhillips Alaska.

White, D., 1988, Oil and Gas Play Maps in Exploration and Assessment: AAPG Bulletin, v. 72, no. 8, p. 944-949.